Viral metagenomics of 100-year-old museum specimens highlights the long-term stability of RNA

Running title: RNA survives well in biological specimens without freezing or fixation

Alexandra H. Keene[1,2] and Mark D. Stenglein[1 *]

1) Center for Vector-Borne and Infectious Diseases, Department of Microbiology, Immunology, and Pathology, College of Veterinary Medicine and Biomedical Sciences, Colorado State University, Fort Collins, CO, USA
2) Quantitative Cell and Molecular Biology Graduate Program

* Correspondence to: Mark.Stenglein@colostate.edu

ABSTRACT

Recovery of virus sequences from old samples provides an opportunity to study virus evolution and reconstruct historic virus-host interactions. Studies of old virus sequences have mainly relied on DNA or on RNA from fixed or frozen samples. The millions of specimens in natural history museums represent a potential treasure trove of old virus sequences, but it is not clear how well RNA survives in old samples. Here, we first experimentally assessed the stability of RNA in insects stored dry at room temperature over 72 weeks. Although RNA molecules grew increasingly fragmented, RNA yields remained surprisingly constant and RT-qPCR of host and virus RNA showed minimal differences between dried and frozen specimens. Next, we acquired *Drosophila* specimens from North American entomological collections to assess RNA survival in much older samples. We recovered sequences from known and novel viruses including several coding complete virus genomes from a fly collected in 1908. We found that the virome of *D. melanogaster* has changed little over the past century. Galbut virus, the most prevalent virus infection in contemporary *D. melanogaster*, was also the most common in historic samples. Finally, we investigated the genomic and physical features of surviving RNA. RNA that survived was fragmented, chemically damaged, and apparently protected by RNA-RNA and RNA-protein interactions. We followed careful protocols to limit contamination from contemporary nucleic acid, and numerous lines of evidence support the conclusion that our results are based on sample-derived sequences. This confirms that RNA - especially certain types of RNA - survives

in biological specimens over extended periods in the absence of fixation or freezing and highlights the utility of dried specimens to provide a clearer understanding of virus evolution.

INTRODUCTION

The study of ancient DNA has been a useful way to better understand the evolutionary history of cellular organisms and their pathogens[1–4]. RNA viruses cause many important diseases, but the study of old RNA has mainly relied on relatively rare fixed or frozen specimens[5,6]. Nevertheless, such specimens have been useful for reconstructing the early history of pandemic pathogens[7,8]. Other studies have taken advantage of endogenized RNA virus sequences, which capture the sequences of viruses that existed long ago [9–11]. The understanding of virus evolution would benefit from the recovery of additional old RNA virus sequences. But how well RNA survives in the absence of freezing or fixation is unclear.

There are reasons to believe that RNA may not survive well over extended periods. For one thing, RNA is short-lived during normal cellular function. The half-life of messenger and ribosomal RNAs are measured in minutes or hours in a living cell[12]. RNA molecules are shorter than genomic DNA and more prone to hydrolysis at physiological conditions[13]. Marketing of RNA-stabilizing reagents further reinforces the idea that RNA is unstable. Studies of historic RNA may therefore be uncommon simply because researchers assume that RNA does not survive well in old specimens.

However, there are an increasing number of studies that indicate that RNA may in fact survive well over long periods[13]. Examples include recovery of a single stranded (ss) RNA virus genome from 750-year-old barley, sequencing of a double stranded (ds) RNA virus genome from 1000-year-old corn, and profiling of RNA from a 130-year-old extinct Tasmanian tiger[14–16]. These studies indicate that RNA can survive for long periods and hint at the potential broad utility of old specimens to study RNA viruses from hundreds or thousands of years ago.

There are nearly 300 million archived arthropod specimens in North American museums alone[17]. Dried beetles, butterflies, ants and fruit flies have yielded useful DNA but to our knowledge RNA has not been sampled from such specimens[18–24]. Amongst the diverse organisms contained in entomological collections are flies in the *Drosophilidae* family[24]. *Drosophila melanogaster* has been instrumental to our understanding of genetics, evolution,

and disease, and the virome of contemporary *D. melanogaster* has been described in detail[25–29].

In this study we used two approaches to investigate RNA survival. First, we experimentally dried and froze flies and mosquitoes and measured RNA yield, length, and detectability over 72 and 52 weeks. Next, we obtained *Drosophila* specimens from museum collections. Using next generation sequencing we characterized surviving viral and host RNA. We recovered viral genome sequences from over 100 years ago and identified properties of RNA associated with survival. We followed strict lab protocols to minimize contamination by contemporary nucleic acid and present many lines of evidence to support the idea that our conclusions are based on RNA from the actual samples. Our findings challenge the assumption that RNA does not survive well and confirm the usefulness of dried biological specimens as a source of RNA to study past viral infection.

RESULTS

Viral and host RNA persisted in dried biological specimens

Entomological collections contain millions of dried specimens, but it's not clear to what extent RNA survives in dried insects, or more generally in dried biological specimens. To assess RNA survival in such samples, we recovered RNA from flies and mosquitoes that had been pinned and stored at room temperature or that had been frozen. We used adult *D. melanogaster* and *Aedes aegypti* from outbred colonies maintained in our insectary[30,31]. Both populations contained individuals persistently infected by one or more viruses. We sampled *D. melanogaster* over 72 weeks and *Ae. aegypti* over 52 weeks. We quantified the concentration and size distribution of recovered RNA and used RT-qPCR to quantify levels of specific host and viral RNAs.

RNA concentrations recovered from individual flies were variable but we were able to recover RNA from all dried samples (**Fig. 1A**). We used a multiple linear regression model (MLR) to assess the relationship between concentration, time and storage condition. There was a small but statistically significant decrease in RNA concentration over time ($F = 4.9$, $p = 0.03$) but surprisingly RNA yields from dried and frozen samples did not significantly differ ($F = 0.84$, $p = 0.36$). We assessed the size distribution of recovered RNA and found that RNA grew

103 increasingly fragmented in both dried and frozen flies (**Fig. 1B, Supp. Fig. 1**). In a multiple
104 linear regression model with the same predictors as above, there was a statistically significant
105 decrease in RNA length over time ($F = 19.8$, $p = 4.3x10^{-5}$) but no significant difference in length
106 between dried and frozen samples ($F = 0.4$, $p = 0.53$).
107
108 Host messenger RNA (mRNA) remained reliably detectable by RT-qPCR in both dried
109 and frozen samples. In *D. melanogaster*, we detected ribosomal protein L32 (RpL32) mRNA in
110 72 of 72 frozen flies and 68 of 72 dried flies (**Fig. 1C**). When we used shorter-range primers
111 that amplified a 56 bp region of RpL32 instead of the 110 bp region amplified by our standard
112 primers, 71 of 72 dried flies were positive (**Fig. 1C**).
113
114 Although there was no statistically significant difference in RNA concentration and length
115 between dried and frozen flies, there was variability in detected levels of specific host and viral
116 RNA targets (**Fig. 1D; Supp. Fig. 2**). Levels of host and viral RNA measured by RT-qPCR
117 decreased as storage time increased. Levels of RpL32 mRNA were higher in frozen flies than
118 they were in the dried flies (**Fig. 1D**).
119
120 Each qPCR run included one positive control: RNA from known infected flies, and three
121 negative controls: an extraction blank (a no sample extraction), a no-sample RT control, and a
122 no template qPCR control. The use of negative controls corresponding to each step of the
123 extraction and detection process would have allowed us to determine when cross-contamination
124 had been introduced if it had been. All controls behaved as expected, confirming the absence
125 of cross-contamination during extraction and RT-qPCR (**Supp. Fig. 3A**).
126
127 The FoCo-17 *D. melanogaster* population we sampled contained individual flies variably
128 infected by galbut virus, La Jolla virus, Nora virus, and Thika virus[32,33]. The prevalence of each
129 virus varied in this outbred population as did viral RNA levels in infected individuals. As with
130 RpL32 mRNA, average levels of detected viral RNAs decreased over time in both dried and
131 frozen flies (**Fig. 1D; Supp. Fig. 2A**). Levels of galbut virus dropped by 69x in frozen samples
132 and 181x in dried samples between 0 and 72 weeks. After 24 weeks, there was no significant
133 difference between galbut virus RNA levels in dried and frozen flies. The overall pattern was
134 similar for the three other viruses (**Fig. 1D; Supp Fig. 2**). Shorter range primers detected galbut
135 virus RNA in fewer qPCR cycles, unsurprisingly confirming that short PCR products work better
136 for fragmented RNA (**Fig. 1E**).

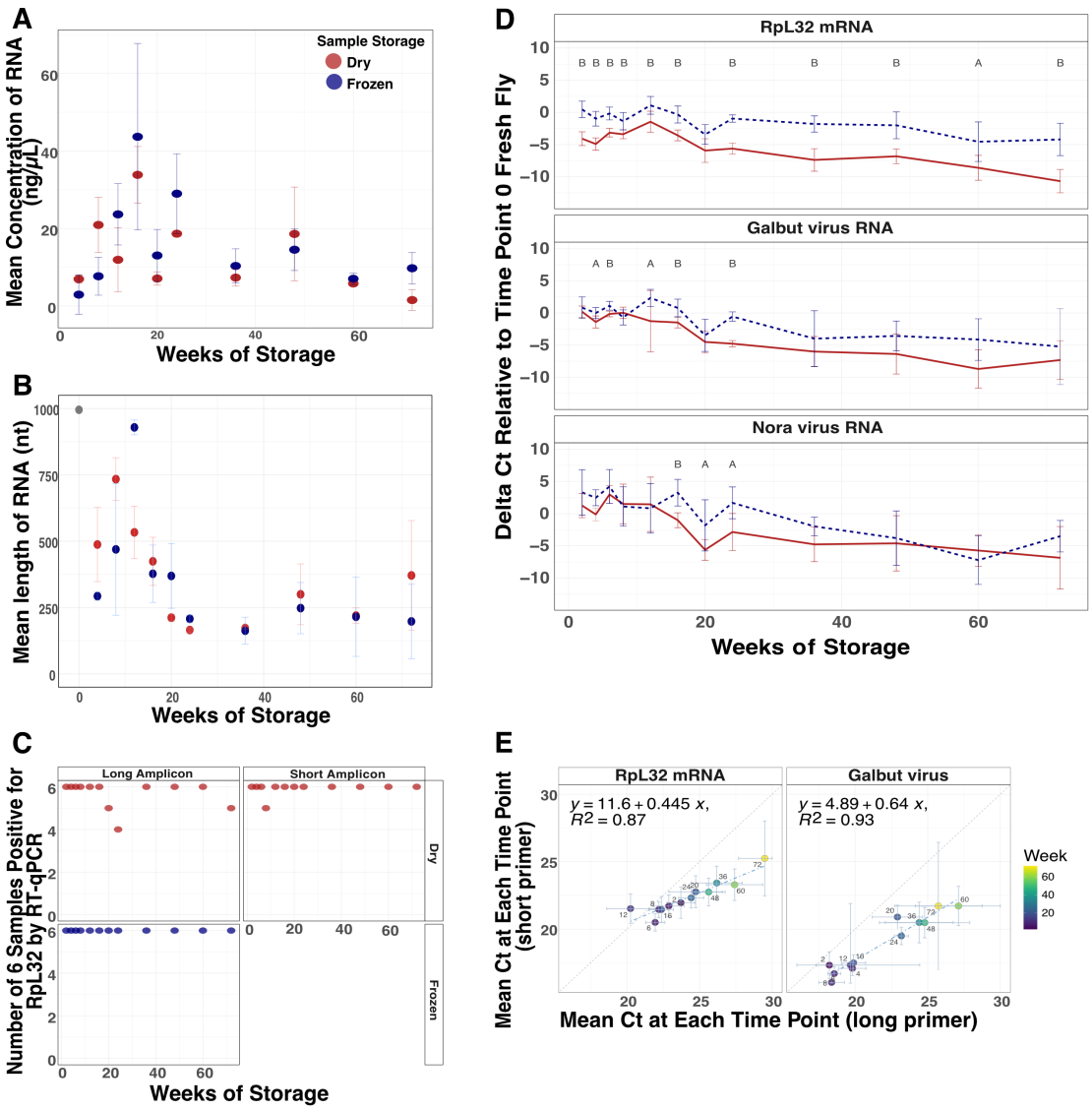

Figure 1: RNA survived in dried flies over 72 weeks. (A) Average RNA concentration and (B) length of RNA from dried and frozen flies over 72 weeks. N = 3 female *D. melanogaster* from each storage condition at each timepoint. (C) Number of samples positive of 3 male and 3 female flies at each timepoint for RpL32 mRNA via RT-qPCR using primers that target long (110 nt) and short (56 nt, dried only) regions of RpL32 mRNA. (D) Average difference of RpL32 mRNA, galbut virus and Nora virus RNA levels relative to fresh *D. melanogaster* collected at the initial timepoint. A two-tailed t-test was used to determine the statistical significance between dried and frozen means at every time point (A < 0.05, B < 0.001). (E) Comparison of mean Ct value at each time point of dried *D. melanogaster* using primers that target a long (x-axis) or

147 short (y-axis) region of RpL32 mRNA and galbut virus. Error bars represent mean plus and
148 minus the standard deviation. N = 3 male and 3 female at each time point.
149
150 RNA also survived well in dried mosquitoes (**Supp. Fig 4**). An MLR was used to assess
151 whether time and/or storage condition impacted mosquito RNA concentration. Over time ($F = 2.09$, $p = 0.15$) and between dried and frozen mosquitoes ($F = 2.37$, $p = 0.13$) there was no
153 statistically significant difference in mosquito RNA concentrations (**Supp. Fig. 4A**). A caveat is
154 that we neglected to save fresh mosquitoes at time 0 as we did with flies, so RNA levels were
155 normalized to levels in the 4-week frozen samples, which had likely already experienced
156 degradation. There was no statistically significant difference in RNA length over time after 4
157 weeks ($F = 0.75$, $P = 0.39$) but there was by storage condition ($F = 79.3$, $p = 2.5\times10^{-13}$; **Supp.**
158 **Fig. 4B**).
159
160 We used RT-qPCR to assess levels and detectability of specific host and viral RNAs in
161 stored mosquitoes. We detected actin mRNA in all 78 dried and all 78 frozen mosquitoes
162 (**Supp. Fig. 4C**). Actin mRNA levels remained consistent over time with no difference between 4
163 weeks and 52 weeks in the frozen samples and a 6x decrease in the dried samples. This
164 mosquito population harbored verdadero virus and Guadeloupe mosquito virus[30,34]. Viral RNAs
165 decreased over time in the dried and frozen specimens. In the dried mosquitoes, virus levels
166 dropped between 13x for verdadero virus and 18x for Guadeloupe mosquito virus between 4
167 and 52 weeks. In frozen mosquitoes there was no difference in verdadero virus levels between
168 4 weeks and 52 weeks but there was a 5x decrease for Guadeloupe mosquito virus (**Supp. Fig.**
169 **4D-E**).
170
171 The mosquito positive and negative controls behaved as expected except for the cDNA
172 positive control sample at week 28, which was negative for Guadeloupe mosquito virus. This
173 may reflect a true negative infection status, given that our cDNA positive control samples were
174 individual mosquitoes from a variably infected outbred population confirmed to have a
175 verdadero virus infection (**Supp. Fig. 3B**).
176
177 ***Drosophila* obtained for RNA metagenomic sequencing were 10-125 years old and from**
178 **entomological collections across the United States and Canada**
179

Having determined that RNA survives well in experimentally dried insects, we turned our attention to much older samples. We obtained 46 specimens from entomological collections across the United States and Canada (**Table 1**). Thirty-two had been assigned as *D. melanogaster* based on morphology, nine as *D. simulans*, and five as unknown drosophilids. Collection dates ranged from 1896 to 2011 (**Fig. 2A; Table 1; Supp. Table 1**). We extracted RNA from 29 specimens following a standard destructive protocol, which yielded RNA concentrations from 0 to 152 ng/μL (**Fig. 2B; Table 1; Supp. Table 1**). Some samples were loaned on the condition that they not be destroyed, so we followed a non-destructive RNA isolation protocol for the remaining samples[35]. This used an overnight incubation with proteinase to liberate internal contents of the specimen while leaving morphology intact. The non-destructive extractions yielded more RNA than the standard protocol ($p = 0.03$), with concentrations ranging from 4 to120 ng/μL (**Fig. 2B; Table 1; Supp. Table 1**). However, when samples from Hawai'i, which had unusually low yields, were removed there was no statistically significant difference between RNA concentration obtained from the two methods ($p = 0.59$; **Supp. Fig. 5**). Four samples that had been stored in 70% ethanol required rehydration prior to extraction (**Supp. Fig 5**).

Table 1: Museum specimen metadata.

Sequencing Based Species ID	Date Collected	Location (1)	Donating Institution	BioSample (2)	Sample ID (3)	Museum Accession	Storage Type	Extraction Method	Concentration (ng/µl) (4)
D. melanogaster	1896	Urbana, IL	Illinois Natural History Survey	SAMN38071661	Illinois_1896	1004284	Dried	Non-Destructive	4
D. melanogaster	1908	Albany, NY	New York State Museum	SAMN38071662	NewYork_1908	-	Dried	Destructive	152
D. melanogaster	1908	Urbana, IL	Illinois Natural History Survey	SAMN38071654	Illinois_1908	1004277	Dried	Non-Destructive	54.6
D. melanogaster	1915	Urbana, IL	Illinois Natural History Survey	SAMN38071656	Illinois_1915_1	1004279	Dried	Non-Destructive	84
D. putrida	1915	Urbana, IL	Illinois Natural History Survey	SAMN38071657	Illinois_1915_2	1004280	Dried	Non-Destructive	6.8
D. melanogaster	1915	Urbana, IL	Illinois Natural History Survey	SAMN38071658	Illinois_1915_3	1004281	Dried	Non-Destructive	12.7
D. melanogaster	1915	Urbana, IL	Illinois Natural History Survey	SAMN38071659	Illinois_1915_4	1004282	Dried	Non-Destructive	16.9
D. melanogaster	1919	St. Paul, MN	University of Minnesota, Insect Collection	SAMN38090828	Minnesota_1919_1	-	Dried	Destructive	0
D. melanogaster	1919	St. Paul, MN	University of Minnesota, Insect Collection	SAMN38071687	Minnesota_1919_2	-	Dried	Destructive	21.6
D. melanogaster	1919	St. Paul, MN	University of Minnesota, Insect Collection	SAMN38071688	Minnesota_1919_3	-	Dried	Destructive	18.9
D. melanogaster	1927	Albany, NY	New York State Museum	SAMN38071663	NewYork_1927	-	Dried	Destructive	21
D. melanogaster	1930	Urbana, IL	Illinois Natural History Survey	SAMN38071660	Illinois_1930	1004283	Dried	Non-Destructive	13.6
D. melanogaster	1942	Glassboro, NJ	Illinois Natural History Survey	SAMN38071655	NewJersey_1942	1004278	Dried	Non-Destructive	10.2
D. melanogaster	1950	Oahu, HI	University of Hawaii, Insect Museum	-	Hawaii_1950_1	-	Dried	Destructive	0
D. melanogaster	1950	Oahu, HI	University of Hawaii, Insect Museum	-	Hawaii_1950_2	-	Dried	Destructive	0
D. melanogaster	1951	Honolulu, HI	University of Hawaii, Insect Museum	-	Hawaii_1951_1	-	Dried	Destructive	0
D. melanogaster	1951	Oahu, HI	University of Hawaii, Insect Museum	-	Hawaii_1951_2	-	Dried	Destructive	0
D. melanogaster	1952	Kauai, HI	University of Hawaii, Insect Museum	-	Hawaii_1952_1	-	Dried	Destructive	0
D. melanogaster	1953	Kauai, HI	University of Hawaii, Insect Museum	SAMN38071677	Hawaii_1953_1	-	Dried	Destructive	0
D. melanogaster	1963	Lebanon Co, PA	Frost Entomological Museum	SAMN38071668	Pennsylvania_1963_1	-	Dried	Non-Destructive	66.4
D. melanogaster	1963	Lebanon Co, PA	Frost Entomological Museum	SAMN38071669	Pennsylvania_1963_2	-	Dried	Non-Destructive	24.4
D. melanogaster	1968	St. Cloud, MN	University of Minnesota, Insect Collection	SAMN38071684	Minnesota_1968	-	Dried	Destructive	13
D. melanogaster	1969	St. Cloud, MN	University of Minnesota, Insect Collection	SAMN38071685	Minnesota_1969	-	Dried	Destructive	38.6
D. melanogaster	1991	St. Cloud, MN	University of Minnesota, Insect Collection	SAMN38071686	Minnesota_1991	-	Dried	Destructive	24.4
D. putrida	2003	Lebanon Co, PA	Frost Entomological Museum	SAMN38071673	Pennsylvania_2003_1	4908	Dried	Non-Destructive	71.2
D. putrida	2003	Lebanon Co, PA	Frost Entomological Museum	SAMN38071672	Pennsylvania_2003_2	4887	Dried	Non-Destructive	13.9
S. pallida	2003	Lebanon Co, PA	Frost Entomological Museum	SAMN38071675	Pennsylvania_2003_3	5867	Dried	Non-Destructive	42
S. pallida	2003	Lebanon Co, PA	Frost Entomological Museum	SAMN38071676	Pennsylvania_2003_4	5873	Dried	Non-Destructive	120
S. pallida	2003	Lebanon Co, PA	Frost Entomological Museum	SAMN38071674	Pennsylvania_2003_5	5863	Dried	Non-Destructive	25.6
D. melanogaster	2006	Davidson, NC	The Davidson College Entomology Collection	SAMN38071666	NorthCarolina_2006_1	-	Dried	Destructive	19.6
D. melanogaster	2006	Davidson, NC	The Davidson College Entomology Collection	SAMN38071667	NorthCarolina_2006_2	-	Dried	Destructive	56.8
D. melanogaster	2006	Davidson, NC	The Davidson College Entomology Collection	-	NorthCarolina_2006_3	-	Dried	Destructive	0
D. melanogaster	2010	Puslinch Township, Ontario, Canada	University of Guelph, Centre for Biodiversity Genomics	SAMN38071680	Canada_2010_1	PHDIP1072-11	Ethanol	Destructive	0
D. simulans	1952	Kauai, HI	University of Hawaii, Insect Museum	-	Hawaii_1952_2	-	Dried	Destructive	0
D. simulans	1952	Kauai, HI	University of Hawaii, Insect Museum	-	Hawaii_1952_3	-	Dried	Destructive	0
D. simulans	1953	Kilauea, HI	University of Hawaii, Insect Museum	SAMN38071678	Hawaii_1953_2	-	Dried	Destructive	0
D. simulans	1958	Maui, HI	University of Hawaii, Insect Museum	-	Hawaii_1958	-	Dried	Destructive	0
D. simulans	1960	Oahu, HI	University of Hawaii, Insect Museum	-	Hawaii_1960	-	Dried	Destructive	0
D. simulans	1963	Lebanon Co, PA	Frost Entomological Museum	SAMN38071670	Pennsylvania_1963_3	-	Dried	Non-Destructive	84.6
D. simulans	1963	Lebanon Co, PA	Frost Entomological Museum	SAMN38071671	Pennsylvania_1963_4	-	Dried	Non-Destructive	48
D. simulans	1965	Oahu, HI	University of Hawaii, Insect Museum	SAMN38071679	Hawaii_1965	-	Dried	Destructive	0
D. simulans	2000	Santa Barbara, CA	Santa Barbara Museum of Natural History	SAMN38071683	California_2000_1	-	Dried	Destructive	17.8
D. simulans	2000	Santa Barbara, CA	Santa Barbara Museum of Natural History	SAMN38071682	California_2000_2	-	Dried	Destructive	55.4
D. simulans	2010	Puslinch Township, Ontario, Canada	University of Guelph, Centre for Biodiversity Genomics	SAMN38071681	Canada_2010_2	PHDIP946-11	Ethanol	Destructive	17.8
D. simulans	2011	Ventura Co, CA	University of Guelph, Centre for Biodiversity Genomics	SAMN38071664	California_2011_1	BBDIV1549-12	Ethanol	Destructive	74.2
D. simulans	2011	Ventura Co, CA	University of Guelph, Centre for Biodiversity Genomics	SAMN38071665	California_2011_2	BBDIV1550-12	Ethanol	Destructive	15.9

(1) All specimens from USA unless otherwise noted
(2) Specimens that did not yield sufficient sequencing library were not sequenced and thus have no BioSample ID
(3) Our study sample ID
(4) RNA concentrations below the limit of detection on the Qubit were assigned a concentration of 0

RNA from samples collected after or before 1960 had average lengths of 159 and 60 nt, respectively (**Fig. 2C**). Although there was variability in RNA quantity and quality, the RNA obtained from these specimens was of suitable length and concentration for downstream analyses.

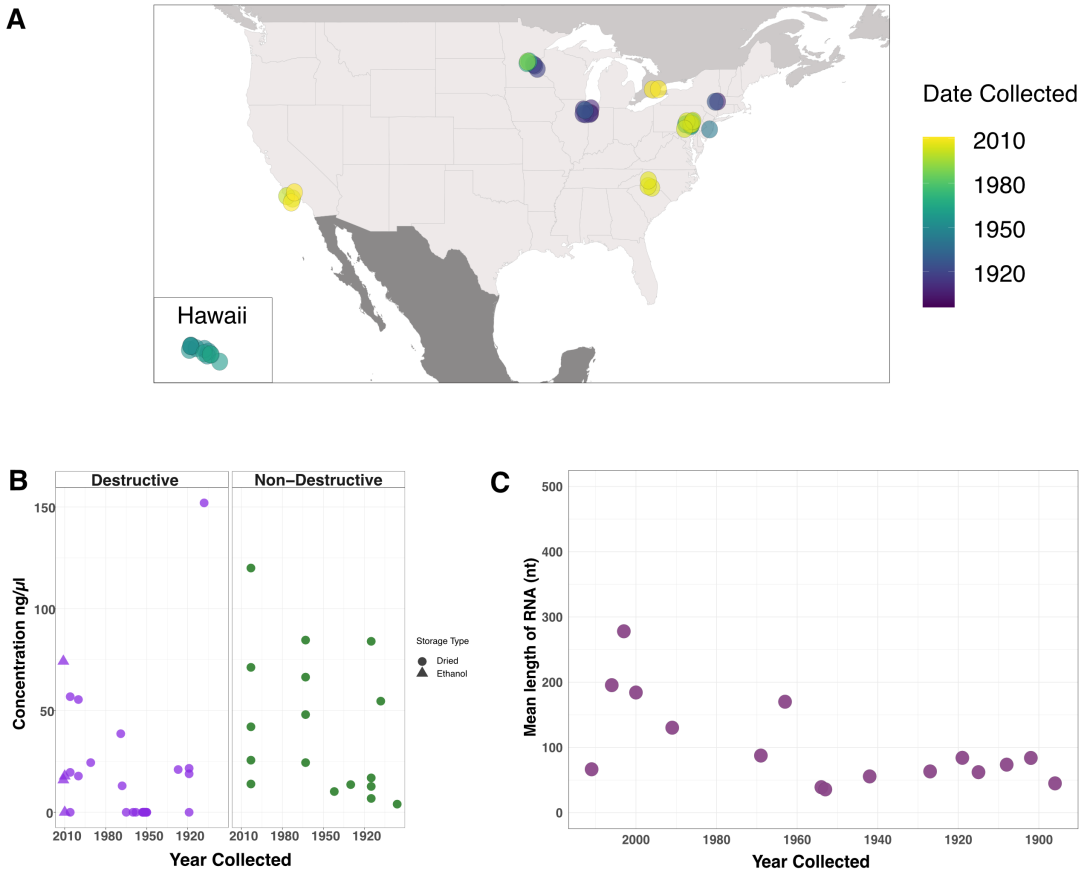

Figure 2: Museum sample collection locations and characteristics of extracted RNA. (A) Map of the United States and Canada indicating sample collection locations. (B) RNA concentration from individual museum flies using either the destructive (purple) or non-destructive (green) extraction method. (C) Mean length of RNA molecules from a subset of museum specimens encompassing the range of years specimens obtained for this study had been collected.

We screened museum samples for galbut virus RNA and RpL32 mRNA using our short-range primers. Sixteen of 46 samples (35%) were positive for galbut virus and 21 (46%) were positive for RpL32 mRNA (**Supp. Fig. 6A, Supp. Table 1**). Positive status was confirmed using melting temperature and agarose gel electrophoresis. The small size of PCR products made them difficult to distinguish from primer dimers on agarose gels, so it is possible that there were false negative calls. All negative control samples were negative as expected (**Supp. Fig. 6B**).

237 **Metagenomic sequencing of museum samples and molecular species assignment**
238
239 We prepared shotgun sequencing libraries from museum sample RNA. Thirty-six
240 samples yielded libraries suitable for sequencing. Sequencing yielded an average of 48 million
241 reads per sample (range: 0.4-238 million). Several samples were sequenced multiple times to
242 increase recovery of complete virus sequences.
243
244 The records for some museum samples did not include morphological taxonomic
245 assignments below the family level, so we used competitive mapping to generate molecular
246 taxonomic assignments. We mapped quality and adapter trimmed reads to a set of 545
247 representative cytochrome oxidase subunit-1 (CO1) sequences from across the Drosophilidae
248 family to generate a molecular species identification for each sample. This molecular species
249 assignment corroborated the museum morphology-based assignment for most samples (**Supp.**
250 **Table 2)**. Four samples labeled as *D. melanogaster* in museum records were revealed to be *D.*
251 *simulans* by CO1-mapping. *D. melanogaster* and *D. simulans* are common, sympatric, and
252 difficult to distinguish morphologically, so such misassignment is expected[36]. Five samples did
253 not have species-level taxonomic assignments from the museums. Of these, CO1-mapping
254 indicated that 2 were *Drosophila putrida* and the remaining three were *Scaptomyza pallida*. One
255 fly collected in Illinois in 1915 was also assigned as *D. putrida* (**Supp. Table 1-2**). These
256 assignments are consistent with the known range of *D. putrida* and *S. pallida*[37]. All fresh frozen
257 and experimental dried samples were assigned as *D. melanogaster* as expected and there were
258 no CO1-mapping reads in the three water negative control datasets.
259
260 **The overall taxonomic composition of new and old samples was similar**
261
262 To broadly assess the source of sequences in our datasets, we taxonomically binned
263 sequences using or lab's metagenomic classification pipeline [38]. This first identified host-
264 derived reads by mapping to an index composed of the *D. melanogaster*, *D. putrida*, and *S.*
265 *pallida* genomes[39,40]. The pipeline then assembled remaining non-host reads and taxonomically
266 assigned the resulting contigs and unassembled reads using a BLASTN search of the NCBI
267 nucleotide database. We tabulated the fraction of reads in each dataset that were assigned to
268 various taxa or that remained unassigned (**Fig. 3**).
269

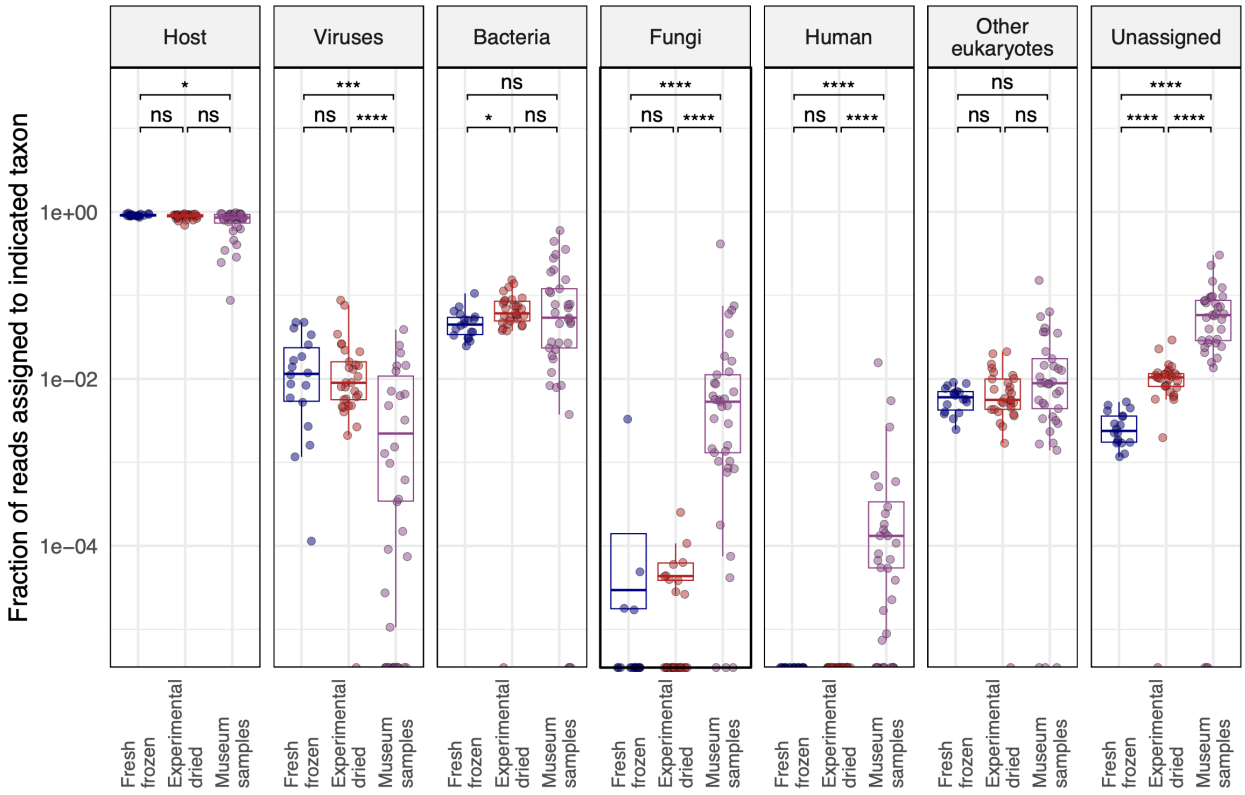

Figure 3: The overall taxonomic composition of old and new samples was similar. The fraction of reads assigned to the indicated taxa are plotted. Each point represents a dataset from an individual fly. Adjusted *p*-values significance levels from Wilcoxon test are indicated. Host-mapping reads were identified by mapping to combined *D. melanogaster*, *D. putrida*, and *S. pallida* genomes. Fractions of reads mapping to other taxa were determined by metagenomic classification of non-host-mapping reads. The "other eukaryotes" category accounts for all eukaryotic taxa apart from fungi and human. Unassigned read fractions account for reads that were not assigned by host-mapping or metagenomic classification.

Most reads mapped to the fly genomes in all datasets, although the median fraction of host-mapping reads fell from 90.5% in fresh samples to 85% in museum samples (**Fig. 3**). This decrease was accompanied by a corresponding increase in unassigned reads. Only 0.2% of reads were unassigned in fresh datasets, compared to 5.5% in museum datasets ($p=2.3\times10^{-6}$). This increase in unassignable reads is likely attributed to the fact that short reads from fragmented RNA contain less information for host mapping or taxonomic assignment. There were on average fewer virus-mapping reads in museum samples, which could reflect the fact that our FoCo-17 population was persistently infected by multiple viruses or could reflect

289 decreased relative survival of viral RNA in old samples. There were increases in the proportion
290 of fungi- and human-mapping reads in museum datasets. Fungal reads in old samples may
291 have derived from saprophytic fungi. Human-mapping reads in museum datasets may have
292 originated from handling of specimens by curators, accumulation of dust on samples, or an
293 increased fraction of contamination-derived sequences in old datasets. The median fraction of
294 human-mapping reads in old datasets was 5.4×10^{-5} and the maximum fraction was 1.6% of
295 reads, in a dataset from Hawai'i. We concluded that some of the reads in our libraries, including
296 human-assigned reads, may have derived from contamination. However, these accounted for a
297 small fraction of datasets and the overall taxonomic composition of new and old datasets was
298 similar (**Fig. 3**).
299
300 **Entomological specimens harbored diverse viral sequences including previously**
301 **unknown viruses**
302
303 We recovered at least one virus sequence from 21 of the 36 sequenced museum
304 samples and two or more virus sequences from 5 samples (**Fig. 4; Table 2**). All but three of the
305 virus sequences corresponded to known *Drosophila*-infecting viruses[25,26]. Galbut virus was the
306 most common virus, with six samples producing coding-complete genomes and six samples
307 producing partial galbut virus genomes (**Fig. 4; Table 2**). The next most common viruses were
308 *D. melanogaster* sigma virus and vera virus, which were detected in three samples each (**Fig. 4;**
309 **Table 2**). The sample with the most viral sequences was collected in 1908 in Illinois, USA: this
310 fly yielded three coding-complete and one partial virus sequence.
311
312 We identified two coding-complete genomes from previously undescribed viruses. The
313 first was a bunyavirus from a *D. melanogaster* collected in Ontario, Canada in 2010, which we
314 named Puslinch virus. The Puslinch virus L protein shares only ~35% pairwise amino acid
315 identity with its nearest known relatives, which were viruses in the genus Herbevirus (**Fig. 4;**
316 **Fig. 5; Table 2**). The other new virus sequence was a sobemo-like virus from a *D. putrida*
317 collected in Pennsylvania, USA in 2003 (**Fig. 4; Fig 5; Table 2**).
318
319 Additionally, we recovered a complete tobacco mosaic virus (TMV) genome with high
320 coverage depth (850x) from the 1908 *D. melanogaster* specimen. We speculated that this
321 sequence may have originated from contamination of the specimen, perhaps during handling by
322 a smoker[41].

Positive control libraries, constructed from RNA from pooled FoCo-17 flies, contained the expected virus sequences (**Fig. 4**). To avoid potential read contamination via index hopping, we sequenced positive control libraries on a separate sequencing run from the museum specimens[42]. Negative control datasets were included in each run and contained fewer than 15k reads after trimming of adapter and low-quality bases. Negative control datasets contained zero reads mapping to any of the virus sequences present in any of the other datasets (**Fig. 4**)[39].

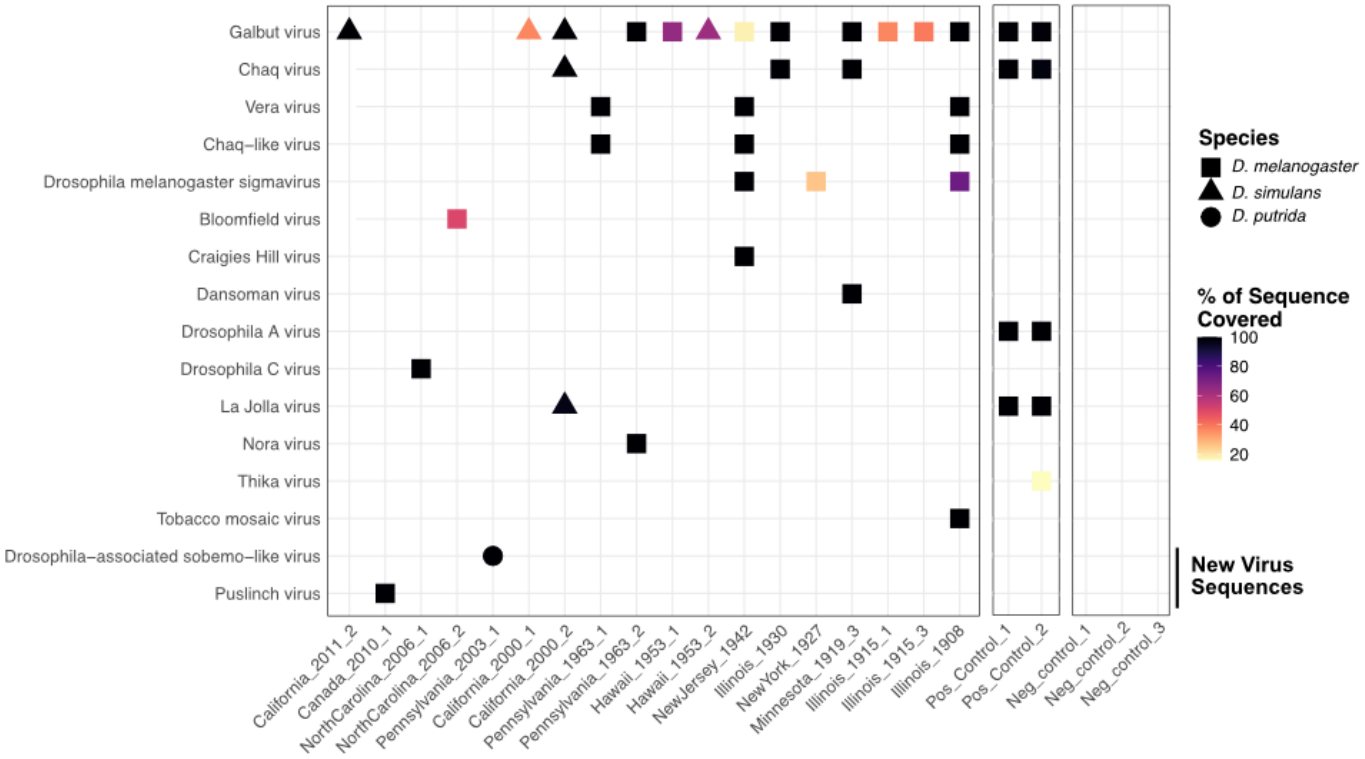

Figure 4. Entomological museum specimens harbored diverse viral sequences. Heatmap showing virus sequences recovered from individual museum samples. Shape corresponds to host species and color corresponds to the percent of reference sequence covered (**Table 2**). For segmented viruses, the average coverage across all segments is shown. Viruses detected in positive control datasets, made from pooled FoCo17 flies, are shown. No reads mapping to any of these viruses were present in any of the three negative control datasets.

340

Table 2: Virus sequences identified in *Drosophila* museum collection specimens.

Date Collected	Location	Sample ID	Virus	GenBank Sequence Accession	Nearest GenBank[1]	% Query Coverage[2,3]	% Identity[4,5]	Completeness	Average Coverage[6]	Estimated Evolutionary Rate[7]
Known										
1908	Illinois	Illinois_1908	Drosophila melanogaster sigmavirus	-	MH384277	73	99.4	Partial sequence	2	-
1908	Illinois	Illinois_1908	Tobacco mosaic virus	OR820564	KY810785	100	99.7	Coding complete sequence	850	7.13E-05
1908	Illinois	Illinois_1908	Vera virus	OR820566, OR820565	MT742171, MT742172	100	99.9 - 100	Coding complete sequence	9-34	1.09E-05 - 0.00E
1908	Illinois	Illinois_1908	Galbut virus	OR820562, OR820561, OR820563	OR729093, MT742165, OR729068	100	98.9 -99.3	Coding complete sequence	7-14	6.43E-05 - 1.00E-04
1908	Illinois	Illinois_1908	Chaq-like virus	OR820560	MT742173	100	99.9	Coding complete sequence	18	6.36E-06
1915	Illinois	Illinois_1915_1	Galbut virus	-	MT742164, MT742161, MT742162	37	96.1	Partial sequence	4	-
1915	Illinois	Illinois_1915_3	Galbut virus	-	MT742164, MT742161, MT742162	39	96.5	Partial sequence	1	-
1919	Minnesota	Minnesota_1919_3	Dansoman virus	OR820572, OR820573	MH384295, MH384270	100	97.4 - 98.3	Coding complete sequence	40-46	2.93E-04 - 3.93E-04
1919	Minnesota	Minnesota_1919_3	Chaq virus	OR820571	MH384367	100	96.9	Coding complete sequence	317	4.11E-04
1919	Minnesota	Minnesota_1919_3	Galbut virus	OR820575, OR820574, OR820576	MT742164, MT742165, OR729068	100	99.4 - 99.6	Coding complete sequence	247-523	4.55E-05 - 9.31E-05
1927	New York	NewYork_1927	Drosophila melanogaster sigmavirus	-	NC_038281	26	99.2	Partial sequence	2	-
1930	Illinois	Illinois_1930	Chaq virus	OR820567	MH384311	100	97.1	Coding complete sequence	32	4.88E-04
1930	Illinois	Illinois_1930	Galbut virus	OR820569, OR820568, OR820570	OR729094, MT742165, OR729070	100	89.3 - 99.7	Coding complete sequence	29-50	3.64E-05 - 1.19E-03
1942	New Jersey	NewJersey_1942	Craigies Hill virus	OR820579, OR820578	MH384377, MH384349	100	90.4 - 98.1	Coding complete sequence	22-40	2.95E-04 - 1.46E-03
1942	New Jersey	NewJersey_1942	Galbut virus	-	MT742164, MT742161, MT742162	18	97.1	Partial sequence	17	-
1942	New Jersey	NewJersey_1942	Chaq-like virus	OR820577	MT742173	100	99.9	Coding complete sequence	490	9.21E-06
1942	New Jersey	NewJersey_1942	Vera virus	OR820582, OR820581	MT742171, MT742172	100	99.9 - 100	Coding complete sequence	463-686	1.58E-05 - 0.00E
1942	New Jersey	NewJersey_1942	Drosophila melanogaster sigmavirus	OR820580	MH384306	100	99.2	Coding complete sequence	46	1.88E-04
1953	Hawai'i	Hawaii_1953_1	Galbut virus	-	MT742164, MT742161, MT742162	65	92.4	Partial sequence	3	-
1953	Hawai'i	Hawaii_1953_2	Galbut virus	-	MT742164, MT742161, MT742162	63	99.7	Partial sequence	3	-
1963	Pennsylvania	Pennsylvania_1963_1	Vera virus	OR820593, OR820592	MT742168, MT742172	100	99.6 - 100	Coding complete sequence	2512-2727	6.55E-05 - 0.00E
1963	Pennsylvania	Pennsylvania_1963_1	Chaq-like virus	OR820591	MT742173	100	99.8	Coding complete sequence	5323	3.64E-05
1963	Pennsylvania	Pennsylvania_1963_2	Galbut virus	OR820588, OR820587, OR820589	MH384303, MH384304, MH384276	100	96.4 - 99.2	Coding complete sequence	8-81	1.73E-04 - 7.98E-04
1963	Pennsylvania	Pennsylvania_1963_2	Nora virus	OR820590	JX220408	100	97.1	Coding complete sequence	16	5.98E-04
2000	California	California_2000_2	La Jolla virus	OR820598	MH384285	97	95.35	Partial sequence	11	5.81E-03
2000	California	California_2000_2	Chaq virus	OR820594	MT742163	100	82.8	Coding complete sequence	62	1.01E-02
2000	California	California_2000_2	Galbut virus	OR820596, OR820595, OR820597	MH384283, MH384336, MH384366	100	83.5 - 92.4	Coding complete sequence	150-271	6.00E-04 - 2.07E-02
2000	California	California_2000_1	Galbut virus	-	MT742164, MT742161, MT742162	37	95	Partial sequence	2	-
2006	North Carolina	NorthCarolina_2006_1	Drosophila C virus	OR820583	OK188767	100	98.3	Coding complete sequence	264	1.86E-03
2006	North Carolina	NorthCarolina_2006_2	Bloomfield virus	-	MF416371, KP714091, KP714093, KP714094	50	99.6 - 100	Partial sequence	0.4-2	-
2011	California	California_2011_2	Galbut virus	OR820600, OR820599, OR820601	MH384283, MH384336, MH384366	100	83.8 - 99.4	Coding complete sequence	16-18	2.00E-03 - 2.61E-02
Novel										
2003	Pennsylvania	Pennsylvania_2003_1	Drosophila-associated sobemo-like virus	OR820603, OR820602	UYL94340.1, QHA33877.1	100	38.1 - 70.6	Coding complete sequence	84-136	-
2010	Ontario, CAN	Canada_2010_1	Puslinch virus	OR820586, OR820585, OR820584	YP_009362026.1, YP_010840683.1, YP_009362024.1	100	32.8 - 39.1	Coding complete sequence	81-188	-

[1] Nearest GenBank sequence is provided for RdRp of Drosophila-associated sobemo-like virus and the L, M and S segment of Puslinch virus.

[2] % Query coverage from BLASTN alignment

[3] % Query coverage from BLASTN alignment for novel virus sequences was determined based on nearest GenBank sequence.

[4] nt, percentage nucleotide identity to closest GenBank sequence identified via BLASTn.

[5] For novel virus sequences, % nt identity to the reference sequence is shown.

[6] Average mapped read coverage across contigs as reported in Geneious.

[7] Calculated using the nearest GenBank sequence with date collected data.

341

342 **Relatedness of old virus sequences to contemporary ones**

343

344 Sequences from museum samples of previously described viruses ranged from 83.5% to
345 100% identical to existing sequences with 38% of the sequences sharing ≥ 99% pairwise
346 identity to existing sequences (**Table 2**). Notably, all vera virus RNA 1 sequences, including one
347 from 1908, were 100% identical to their closest available existing sequence, though the vera
348 virus RNA 2 and chaq-like sequences from the same samples were not identical to existing
349 sequences.

350

351 We initially considered a Bayesian approach to generate evolutionary rate estimates but
352 found our data had insufficient temporal signal[43]. We instead generated initial estimates of
353 evolutionary rates using differences in sequence identity and sampling times for the most
354 closely related contemporary sequences (**Supp. Fig. 7; Table 2,**). This may underestimate
355 rates due to saturation and might overestimate rates because the old sequences are likely not
356 the direct ancestors of the contemporary sequences[44–46]. Sequences without a suitably similar
357 contemporary sequence (e.g., USA 2000 and 2011 galbut virus *D. simulans* RNA 2 and 3) were
358 not analyzed in this way. Estimated rates were generally higher in sequences from more recent
359 samples (2000-2011) and lower in sequences from older samples, with sequences from 1908
360 showing the lowest rates (**Supp. Fig. 7**). This observation is consistent with the time-dependent
361 rate phenomenon, in which evolutionary rate estimates decrease as the timescale of
362 measurement increases[44,47].

363

364 The most common contemporary viral infection of *D. melanogaster* is galbut virus, the
365 success of which is likely attributable to efficient biparental vertical transmission and minimal
366 apparent fitness costs[26,30,48]. Detection of galbut virus in museum samples by sequencing
367 matched detection by RT-qPCR (**Table 1**). In maximum likelihood trees, three clades of galbut
368 virus were evident: two clades (A and B) consisted of sequences from *D. melanogaster* while
369 the third clade consisted of sequences from *D. simulans* (**Fig. 5A-C**). An endogenized galbut
370 virus RNA 1 sequence was on its own branch most closely related to clade A (**Fig. 5A**)[49]. All the
371 historic galbut virus sequences fell within existing galbut virus diversity and clustered with other
372 sequences from the same host i.e., the two *D. simulans* sequences clustered with previously
373 described *D. simulans* sequences and the *D. melanogaster* sequences with known *D.*
374 *melanogaster* RNA1 sequences (**Fig. 5A**). Interestingly, the RNA1 and RNA2 sequence from
375 Illinois 1930 clustered with clade A but this virus's RNA 3 was situated on a separate branch.

The 1930 Illinois RNAs 1 and 2 were 99% identical to contemporary sequences in GenBank while RNA 3 was only 89% identical. This phylogenetic discordance is consistent with galbut virus reassortment[50].

The sigma virus sequence from 1942 clustered within the previously described diversity of *D. melanogaster* sigma viruses (**Fig. 5D**). Puslinch virus and *Drosophila*-associated sobemo-like virus sequences were situated on their own branches on trees of related sequences (**Fig. 5E-F**). These new virus sequences are highly divergent and may establish new genera or higher order taxa.

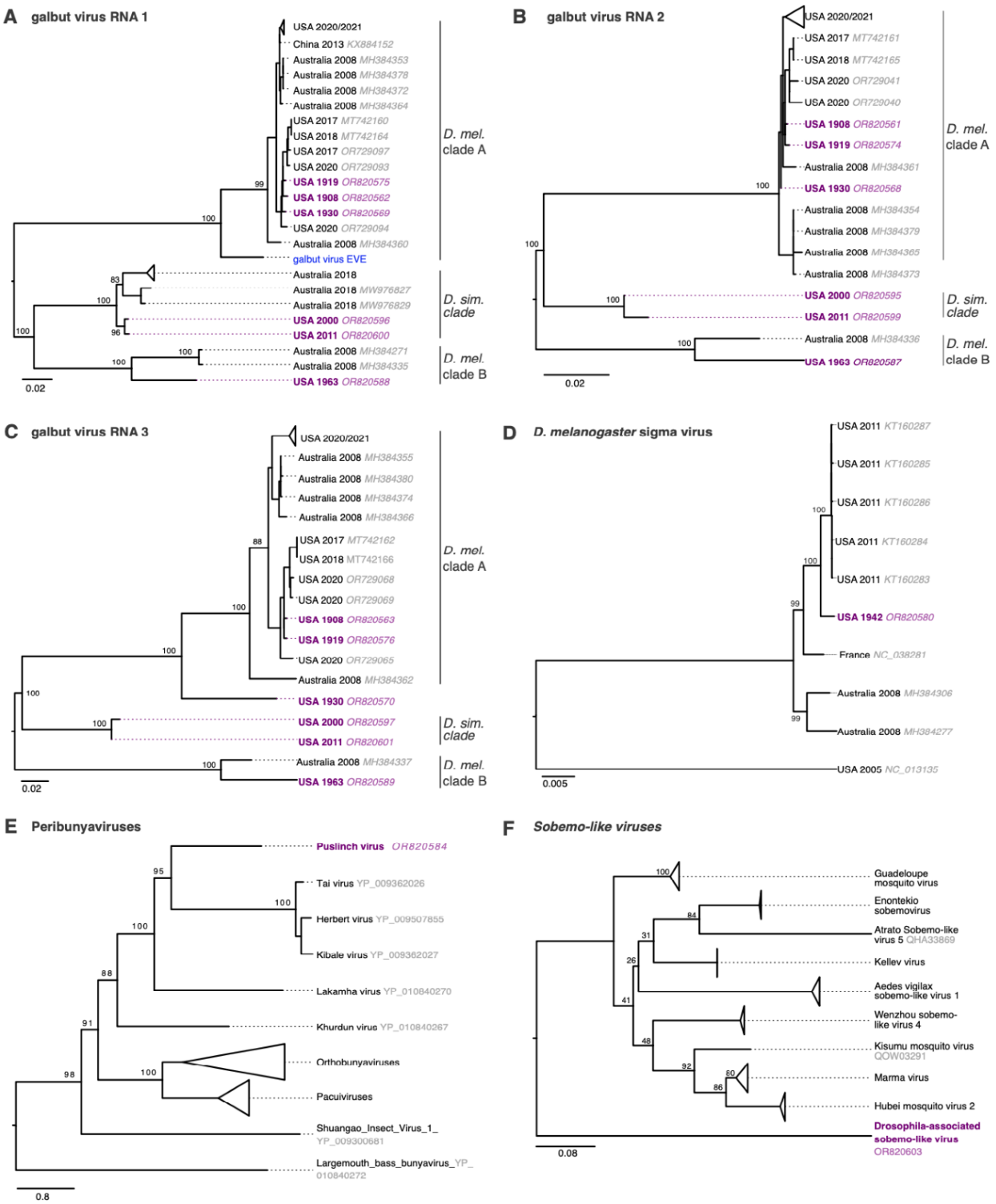

Figure 5: Trees showing museum sample virus sequences in the context of related contemporary sequences. (A) Maximum likelihood trees for galbut virus RNA 1 (RdRp) sequences, (B) galbut virus RNA 2 sequences, (C) galbut virus RNA3 sequences, (D) *D. melanogaster* sigma virus sequences, (E) L protein sequences for viruses in the family

390 *Peribunyaviridae*, and (F) putative RNA-dependent RNA polymerase protein sequences related
391 to the new *Drosophila*-associated sobemo-like virus. Trees in (A)-(D) are based on nucleotide
392 alignments and trees in (E) and (F) are based on protein sequence alignments. Purple color
393 indicates museum sample-derived sequence generated in this study. Accession numbers are
394 noted except when groups of closely related sequences are collapsed. All trees are midpoint
395 rooted. Blue tip indicates the sequence of an endogenized galbut virus RNA 1 sequence.
396
397 **Certain types of RNA survived better in old samples**
398
399 We performed a variety of analyses to characterize the molecular and genomic
400 properties of surviving RNA. An initial indication that not all types of RNA survived equally
401 came from the strandedness of virus-mapping reads. We constructed libraries using a protocol
402 that preserved information about the RNA strand from which reads derived[51]. Galbut virus is a
403 partitivirus, which have dsRNA genomes[52]. But in infected flies, nearly all galbut virus RNA was
404 positive (+) sense (98.2% in fresh frozen flies; **Fig. 6; Supp. Fig. 8**). This is presumably
405 because most galbut virus RNA in infected cells is messenger RNA (mRNA). The fraction of
406 +strand galbut virus RNA decreased in older samples. In experimentally dried samples an
407 average of 89.1% of reads were from +strand RNA, and this value fell to 74.1% in museum
408 specimens ($p = 1.4x10^{-4}$; **Fig. 6**). The decreasing fraction of +strand galbut virus RNA could be
409 explained by the preferential survival of double-stranded galbut virus RNA in older samples.
410
411 Coverage of galbut virus in museum datasets derived from all segments and was not
412 concentrated in regions of RNA 1 corresponding to the PCR primers we use to detect galbut
413 virus in our lab (**Supp. Fig. 8**). The lack of higher coverage in PCR product regions supports the
414 conclusion that galbut virus sequences did not result from contamination by contemporary PCR
415 products.
416
417 Other viruses had different fractions of +strand RNA that were consistent with the
418 genome type of each virus (**Fig. 6**). For instance, a majority of reads from *D. melanogaster*
419 sigma virus, a negative (-) strand RNA virus, were from -strand RNA[29]. RNA from Nora virus (a
420 +strand virus) remained almost totally +strand in all samples[33]. The fraction of +strand vera virus
421 RNA, another partitivirus, remained high in old samples (**Fig. 6**). This indicated that it was not
422 simply dsRNA that survived in older samples.
423

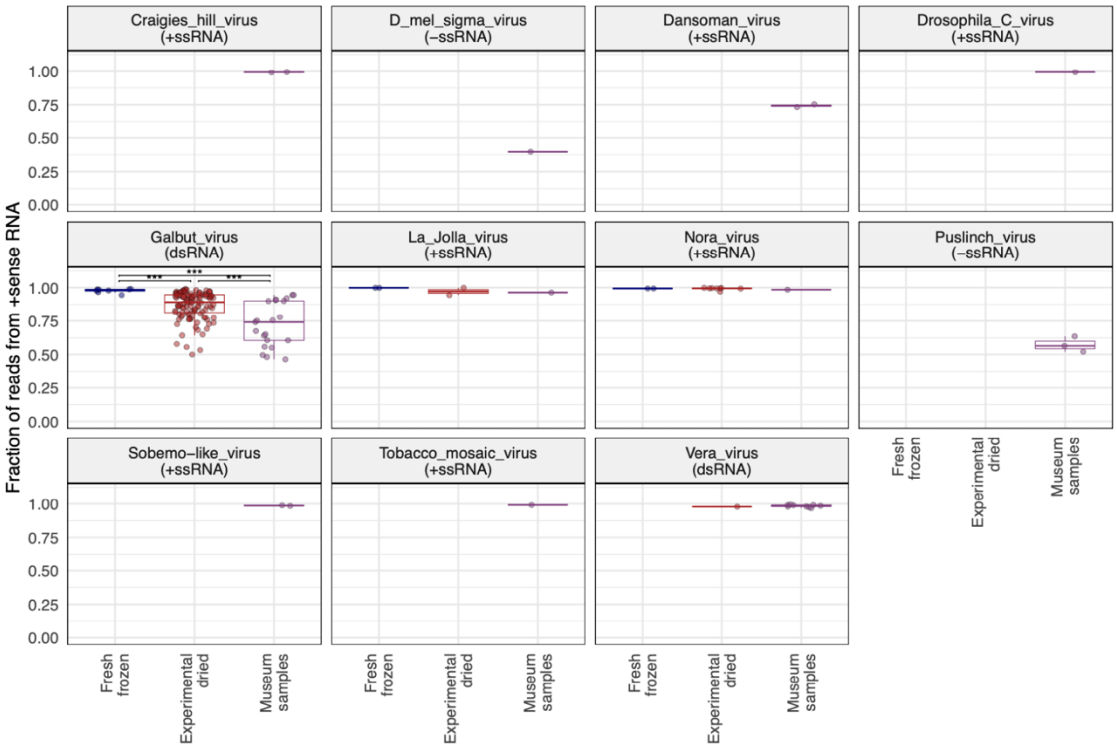

Figure 6: The strandedness of galbut virus RNA in old samples is consistent with preferential survival of dsRNA. The fraction of virus-mapping reads that originated from +strand RNA is plotted. Each point represents a dataset from an individual *D. melanogaster* fly. Significance levels of Wilcoxon test adjusted *p*-values are indicated: ns: p > 0.05; *: p <= 0.05; **: p <= 0.01; ***: p <= 0.001; ****: p <= 0.0001. Vera virus and other viruses were not present in sufficient numbers in different datasets to statistically evaluate how their strand ratios changed over time.

Nevertheless, there was additional evidence from host-mapping reads that double-strandedness contributed to preferential RNA survival. Most host-mapping RNA derived from ribosomal RNA (rRNA), and most rRNA-mapping reads derived from the +strand (**Fig. 7**). In fresh samples, there was on average 698x more +strand rRNA than -strand rRNA. The small amount of -sense rRNA could have derived from anti-sense transcription of rRNA genes or pseudogenes[53]. In experimentally dried and museum samples, the +strand:-strand rRNA ratio dropped to 142:1 and 30:1, respectively ($p = 8.2 \times 10^{-13}$ and 2.8×10^{-22}; **Fig. 7**). This drop was driven by a relative decrease in +strand rRNA and a relative increase in -strand rRNA in older samples (**Supp. Fig. 9**). This pattern could be explained by the preferential survival of sense:antisense rRNA duplexes. However, even in old samples, there was 30x more +strand

443 rRNA than –strand (**Fig. 7**), so sense:antisense duplexes could not account for all surviving
444 rRNA.
445

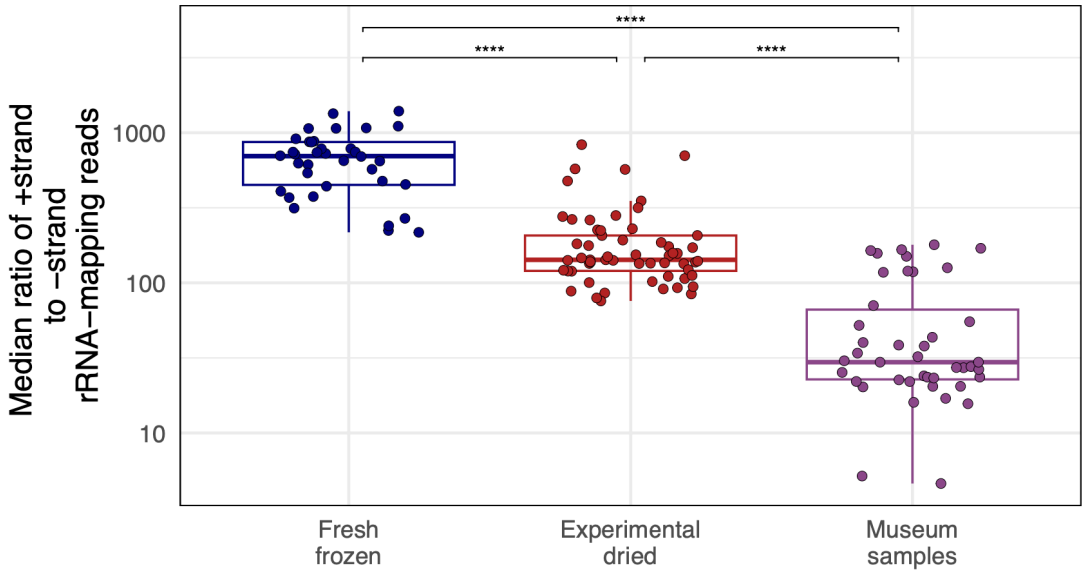

446
447 **Figure 7: Strand ratios of surviving ribosomal RNA were consistent with preferential**
448 **survival of dsRNA**. The median ratio of +strand to –strand coverage of rRNA-mapping
449 reads. Points represent individual-fly datasets. Adjusted *p*-values significance levels from
450 Wilcoxon test are indicated.
451
452 Coverage levels across rRNAs varied more in old samples than they did in new
453 samples, where coverage was relatively even (**Fig. 8**). For instance, coverage surrounding
454 position 1500 of the 18S rRNA and position 3000 of the 28S rRNA had consistently lower
455 coverage in old samples (**Fig. 8**). In contrast, in fresh samples coverage over these same
456 regions was similar to average coverage.

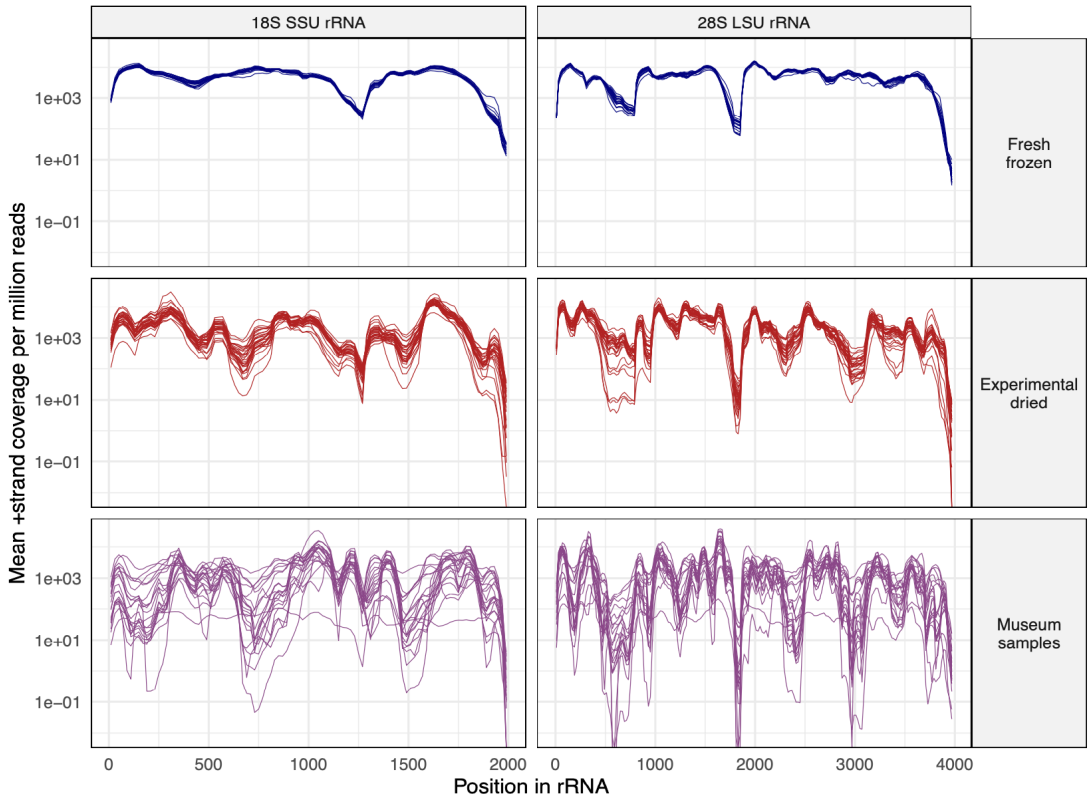

Figure 8: Certain regions of ribosomal RNA were underrepresented in old samples. The mean +strand rRNA coverage per million reads in 20 bp windows is plotted for *D. melanogaster* datasets. Each line represents a dataset from an individual fly. SSU: small subunit (18S) rRNA; LSU: large subunit (28S) rRNA.

To investigate why some rRNA regions might not survive as well as others, we took advantage of a high resolution cryo-electron-microscopy structure of the *D. melanogaster* 80S ribosome[54]. This structure includes ribosomal proteins and RNA (**Fig. 9A**). It is possible to resolve individual rRNA bases in the structure and to determine whether they are interacting with other bases, and whether they are present in the structure (**Fig. 9B**). We used this structure and RNApdbee software to individually assign the 5965 rRNA bases to one of four categories: paired with other rRNA bases (62.9%), unpaired (29.2%), present in higher-order secondary structures like pseudoknots (4.5%), or missing from the 3D structure altogether (3.4%; **Fig. 9B**) [54–56].

We calculated coverage of bases in each of these four categories relative to total median coverage (**Fig. 9C**). Paired bases had higher average coverage in older samples (p =

476 1.9×10^{-19} in museum samples vs. fresh ones). Similarly, bases in higher-order secondary
477 structures like pseudoknots had higher coverage in old samples ($p = 3.3 \times 10^{-17}$ relative to fresh).
478 In contrast, unpaired bases had lower average coverage in old samples ($p = 3.8 \times 10^{-20}$ vs. fresh
479 samples). Bases that were not captured in the 3D structure were the least well represented in
480 older samples, with coverage levels 8x lower than overall average coverage in museum
481 samples ($p = 1.0 \times 10^{-19}$ relative to fresh frozen). Experimentally dried sample coverage levels
482 were generally intermediate between fresh and museum samples, consistent with their
483 intermediate age (**Fig. 9C**).
484
485 These patterns suggested that the molecular environment surrounding rRNA bases
486 influenced the likelihood that they would survive. Being base-paired or in a higher-order RNA
487 secondary structure protected bases, enabling them to survive over longer periods. In contrast,
488 unpaired bases or bases not present in the 3D structure - presumably because they were
489 outside of the protective environment of the ribosome - were less likely to survive.

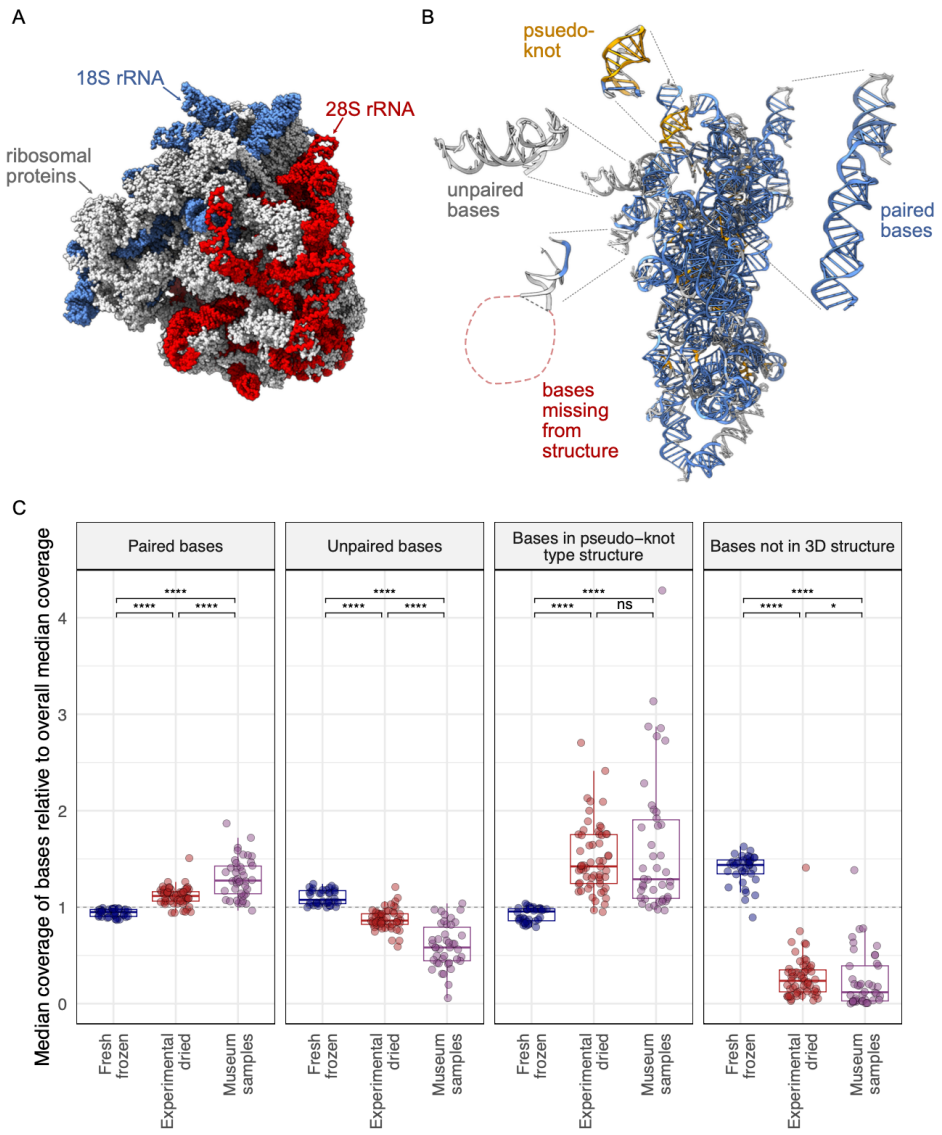

Figure 9: **Different types of ribosomal RNA exhibited differential survival in old samples.** (A) The structure of the *D. melanogaster* 80S ribosome from Anger at al, showing ribosomal proteins and the 18S and 28S ribosomal RNAs. (B) The 18S rRNA with individual bases color coded to indicate whether they are paired with other rRNA bases (blue), unpaired (grey), or involved in higher order pseudo-knot type structures (gold). Some bases were not captured in the structure (red). Bases were binned into categories using RNApdbee software. The 18S rRNA is rotated relative to panel A. (C) The median coverage level of bases in the indicated categories relative to total median coverage is plotted. Each point represents a dataset from an individual *D. melanogaster* fly. Significance levels of Wilcoxon test adjusted *p*-values are indicated.

501

502 **Different types of non-ribosomal RNA survived differentially in old samples**

503

504 We also quantified the extent to which different types of non-ribosomal host RNA
505 survived in old samples. We mapped reads from *D. melanogaster* samples to the *D.*
506 *melanogaster* genome and used the ALFA software to quantify the different types of host RNA
507 present in each dataset[57]. ALFA combines mapping information with genome annotation to
508 assign mapped reads to one of a dozen RNA types (**Fig. 10**). As expected, most reads were
509 categorized as rRNA, though there was relatively less rRNA in older samples (**Fig. 10A**; $p =$
510 5.1×10^{-6} for museum vs. fresh samples). There was also relatively less protein-coding mRNA in
511 older samples (**Fig. 10B**; $p = 5.7 \times 10^{-4}$). Opposite strand RNA levels – that is, reads derived from
512 the RNA strand opposite an annotated feature - were elevated in older samples, consistent with
513 the preferential survival of sense:antisense transcript duplexes ($p = 1.8 \times 10^{-7}$). Highly structured
514 transfer RNA (tRNA) levels were also elevated in older samples ($p = 5.9 \times 10^{-5}$)[58,59].

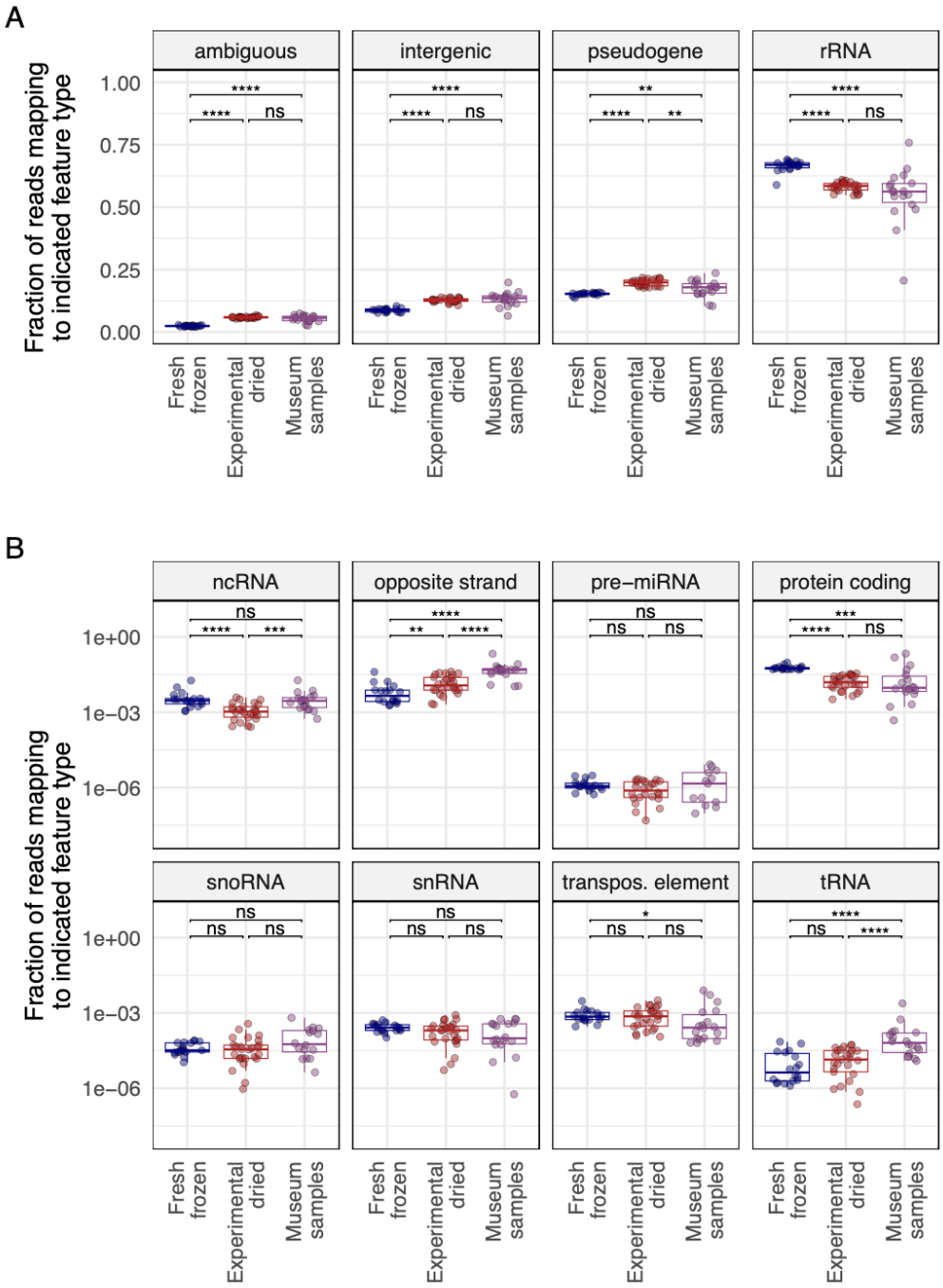

Figure 10: **Certain types of RNA survived better in old samples.** The fraction of reads in *D. melanogaster* datasets mapping to the indicated RNA types is plotted. Each point represents a dataset from an individual fly. Adjusted *p*-values significance levels from Wilcoxon test are indicated. (A) Types of RNA present at >5% median abundance. (B) Types of RNA present at <5% abundance. Abbreviations for different RNA types: ncRNA: non-coding RNA; miRNA: micro RNA; snoRNA: small nucleolar RNAs; snRNA: small nuclear RNA; tRNA: transfer RNA.

522 **Old RNA was chemically damaged**

523

524 Old DNA molecules are fragmented and chemically damaged[60]. Polymerases can
525 misincorporate bases when copying damaged templates, causing damage to manifest as
526 substitutions in library molecules[61–63]. For example, deaminated cytosines, common in ancient
527 DNA, result in C-to-T substitutions in library molecules. In fact, signatures of chemical damage
528 in sequence reads are taken as evidence that reads derive from old DNA and not from
529 contaminating contemporary DNA.

530

531 We quantified mismatch patterns in mapped reads to look for signatures of chemical
532 damage in old RNA (**Fig. 11**). Mismatch frequencies varied in different sample types. Some
533 differences in mismatch frequencies could be attributed to samples being sequenced on
534 different sequencing runs (we sequenced museum samples separately from other samples to
535 avoid the possibility of read misassignment from index-hopping) [64]. The largest difference
536 between old and new samples was an elevated frequency of C-to-T substitutions in reads from
537 museum samples. The median level of C-to-T mismatches in datasets from museum samples
538 was 40x higher than in fresh-frozen datasets (2.0×10^{-3} frequency of C-to-T mismatches vs.
539 5.0×10^{-5} (**Supp. Fig. 10**; $p=1.0 \times 10^{-10}$). This increased frequency of C-to-T substitutions is
540 consistent with deamination of cytosines in old RNA.

541

542 A-to-G substitutions were the next most elevated type of mismatch in old samples (**Fig.**
543 **11**). A-to-G substitutions occurred at a rate 4.4-fold higher in museum samples than in fresh
544 datasets (5.7×10^{-4} vs. 1.3×10^{-4}; $p=1.6 \times 10^{-10}$). Such substitutions can result from spontaneous
545 deamination of adenine to hypoxanthine[60,65].

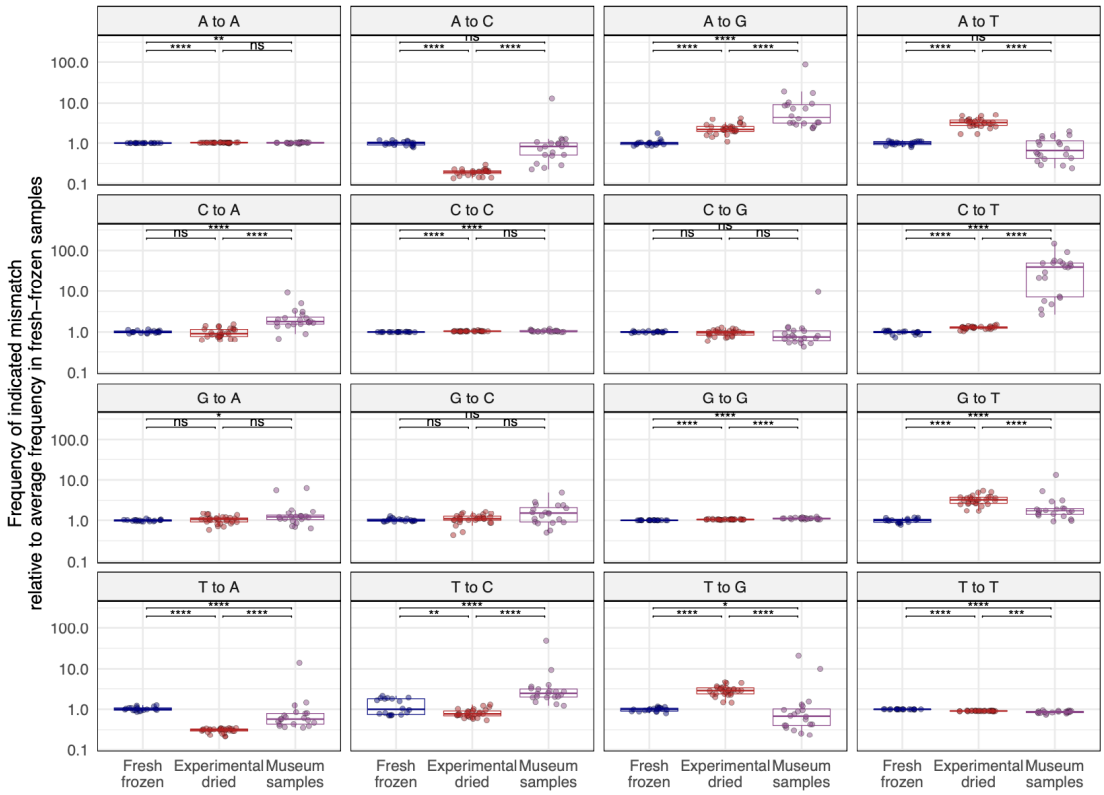

Figure 11. Old RNA was chemically damaged and exhibits mismatch patterns consistent with cytosine and adenine deamination. Mismatches in rRNA-mapping reads from *D. melanogaster* datasets were quantified and the frequency of each mismatch type relative to the median frequency in fresh-frozen datasets is plotted. Each point represents a dataset from an individual fly. Adjusted *p*-values significance levels from Wilcoxon test are indicated.

Host-mapping reads exhibited species specificity

We took advantage of the fact that our musuem samples derived from 4 different species to investigate the possibility that host-mapping reads – specifically rRNA-mapping reads – might result from contemporary contamination. The likely source of fly-mapping contamination would be the *D. melanogaster* that we rear and study in our lab[48]. The 18S and 28S ribosomal RNA sequences of *D. melanogaster* and *D. simulans* share over 99% pairwise identity which makes them difficult to distinguish by competitive read mapping. We therefore collected and mapped reads to the relatively variable region of the ribosomal RNA between the 18S and 5.8S genes (the internal transcribed spacer 1, ITS) of the 4 fly species that we sampled (**Table S1**; **Fig. 12; Supp. Fig. 11**). All ITS-mapping reads in museum datasets mapped to the expected species ITS sequence and no reads mapped to an unexpected species (**Fig. 12**). Positive and

negative control samples behaved as expected, with water negative control datasets containing no reads mapping to any of these 4 ITS sequences (**Supp. Fig. 11**). If fly rRNA-mapping reads were from contamination, we would have expected there to be *D. melanogaster*-mapping reads in the non-*melanogaster* and negative control datasets; instead, there were none. The perfect concordance of ITS mapping and sample species supported the conclusion that the host-mapping reads in our datasets were indeed from museum samples.

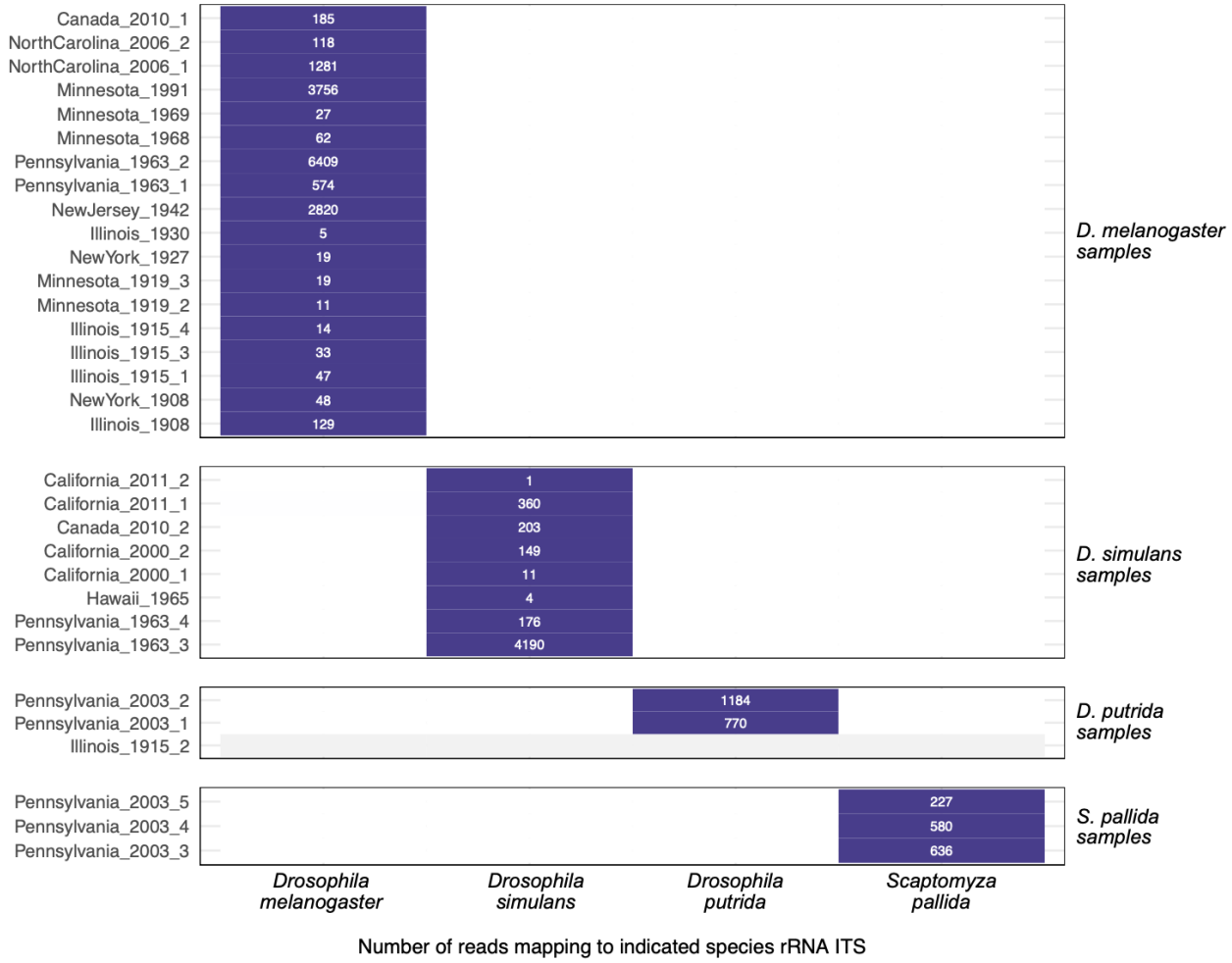

Figure 12: Host-mapping reads exhibited species specificity. The number of reads mapping to the indicated species rRNA internal transcribed spacer 1 (ITS) sequence for each museum sample dataset is shown. Samples are grouped according to their molecular species assignment (**Table S1**). Datasets with no ITS-mapping reads are represented with grey.

DISCUSSION

580

581 In this study we took a two-pronged approach to investigate RNA stability in old
582 biological samples. In flies and mosquitoes stored dry at room temperature for weeks or
583 months, RNA grew increasingly fragmented, but RNA yields did not significantly decrease, and
584 cellular and viral RNA remained detectable. Perhaps the most unexpected result from this
585 experiment was the limited difference in RNA quality and quantity between dried and frozen
586 samples (**Fig. 1; Supp. Figs. 2, 4**). We recovered RNA from dried flies that were from as far
587 back as the 1890s and used this RNA to make sequencing libraries. We recovered coding
588 complete virus sequences from 11 old specimens and identified two novel virus sequences. We
589 also showed that certain types of RNA tended to survive in old samples, including dsRNA and
590 RNA in secondary structures or ribonucleoprotein complexes.
591

592 There were limitations to the experimental arm of our study. First, RNA recovery from
593 individual flies and mosquitoes - even fresh ones - was variable. Second, we used outbred
594 populations of flies and mosquitoes with different levels of virus infection between individuals. In
595 future studies, optimization of our RNA isolation protocol to decrease yield variability between
596 individual flies and mosquitoes would be useful. It would also be better to use pinned specimens
597 from inbred populations with less variable infection phenotypes.
598

599 We found that not all RNA survived equally well and described molecular features that
600 influenced how well different types of RNA survived. dsRNA survived better than ssRNA.
601 Surviving RNA duplexes derived from intermolecular base pairing, such as sense-antisense
602 duplexes (**Figs. 6, 7A, 10B**) and from intramolecular base pairing, such as paired rRNA bases
603 (**Fig. 9C**). The preferential survival of dsRNA likely reflects decreased susceptibility to
604 hydrolysis[66]. However, double strandedness could not explain all RNA survival, as RNA from
605 certain viruses remained largely +strand (**Fig. 6**) and unpaired rRNA survived (albeit less than
606 paired rRNA; **Figs. 7, 9**). It may be that ribonucleoprotein complexes like virus particles and
607 ribosomes provide a protective environment in which RNA can survive longer.
608

609 Like old DNA, old RNA was fragmented and chemically damaged (**Figs. 2C, 11**). And,
610 like DNA, deamination was the most evident type of damage (**Fig. 11**). Other types of damage
611 may be common in old RNA but undetectable by sequencing. The extent to which
612 ribonucleases, deaminases, and other enzymes involved in normal RNA processing continue to

613 function in dead cells is unclear, but it is likely that most RNA fragmentation and damage in old
614 samples results from spontaneous chemical rather than enzymatic degradation.
615
616 Environmental factors like temperature and humidity likely play a major role in the
617 survival of RNA. It was notable that none of the 12 specimens from tropical Hawai'i yielded
618 enough RNA to be detected fluorometrically and only two generated sequenceable libraries
619 (**Fig. 2b, Table 1 & Supp. Fig. 5**). Humidity might be more important than temperature, as RNA
620 was recovered from 1000-year-old corn in Arizona, where temperatures fluctuate to extremes,
621 but humidity is very low[15]. If this were true, RNA might survive better in drier environments and
622 in quickly desiccating samples like the small insects that are the focus of this work. Even for
623 much larger samples like wooly mammoths, dehydration has been proposed to promote
624 preservation of nuclear architecture and biological macromolecules[67].
625
626 The virus sequences we recovered revealed that the *D. melanogaster* virome has not
627 changed much over the last 120 years. All the viruses that we detected in *D. melanogaster*,
628 except for Puslinch virus, had already been described in contemporary *D. melanogaster*[25,26]. For
629 the most part the old sequences were closely related to contemporary sequences (**Table 2**). For
630 example, the viruses infecting the fly collected in 1908 were >98% identical to known *D.*
631 *melanogaster* viruses (**Fig. 4; Table 2**).
632
633 The discrepant phylogenetic positions of the 1930 galbut virus segments is consistent
634 with reassortment[68]. The 1930 galbut virus RNA 3 sequence that is positioned on its own branch
635 may correspond to an extinct RNA 3 lineage, or simply one that has not been sampled before
636 (**Fig. 5C**). Similarly, the endogenous galbut virus RNA 1 sequence in these trees may represent
637 an extinct lineage or an ancestor of contemporary galbut virus RNA 1 sequences (**Fig. 5A**)[49]. A
638 potential benefit of large-scale sequencing of old samples is that it could provide estimates of
639 how frequently virus lineages go extinct from a particular host.
640
641 Contamination from contemporary nucleic acid has been a long-standing concern for
642 those sequencing ancient DNA[69]. There was evidence of low-level contamination in our
643 datasets (**Fig. 3**), and it is difficult to completely avoid contamination in NGS datasets, even
644 when sequencing new samples[70,71]. But, there were numerous lines of evidence to support the
645 idea that our conclusions were based on sequences from actual old RNA and not from
646 contemporary contamination. Old RNA was short and chemically damaged; properties that are

shared with old DNA[60]. Characteristics of RNA from experimentally dried samples were generally intermediate between those of fresh RNA and museum RNA, consistent with their intermediate age (**Figs. 6-11**). We recovered different virus sequences from different old samples, and reads in individual datasets supported the same distinct virus sequences (**Table 2**). The virus sequences we recovered were for the most part known *Drosophila*-infecting viruses. Although many virus sequences from old samples were similar to existing contemporary sequences, most were not identical (**Table 2**). The exceptions were three vera virus RNA 1 sequences that were identical to existing sequences. But the RNA 2 and chaq-like sequences from these samples were not identical to any contemporary sequences. The two new virus sequences we recovered were divergent, but their closest relatives were from other insects (**Table 2; Fig. 5**). The tobacco mosaic virus sequence from the 1908 dataset was an exception, which we can't explain except to suggest that this specimen was contaminated during handling by a smoker, as individual cigarettes were found to contain as many as 10^9 TMV RNA copies[41]. There was no peak in galbut virus coverage corresponding to our diagnostic RT-qPCR amplicons, which would be a prime candidate source of contaminating galbut virus sequences (**Supp. Fig 6**)[30,48]. All museum samples that were positive for galbut virus by RT-qPCR and generated a sequenceable library were also positive by sequencing (**Supp. Table 1**). Negative control datasets were uniformly free of virus and rRNA-mapping reads (**Fig. 4**; **Supp Fig. 11**). Galbut virus sequences from *D. simulans* museum samples clustered with contemporary *D. simulans* sequences, and the same for *D. melanogaster* sequences (**Fig. 5**).

Indeed, the species-specificity of host and virus sequences (**Figs. 5 & 12**) provides some of the strongest support for the idea that our analyses are based on nucleic acid from the actual old samples. If our conclusions were based on contaminating contemporary sequences, it would be necessary to invoke a complicated mechanism where contaminating host and virus nucleic acids sorted themselves by species into each sample (**Figs 5 & 12**). The overall apparent lack of contaminating virus and host sequences was consistent with the fact that all extractions were done in biosafety cabinets following a pre-PCR to post-PCR workflow, including DNase treatment before RT-qPCR and library preparation.

RNA can persist in biological samples over decades or centuries without freezing or fixation. The half-life of RNA in dead cells is clearly much longer than in living cells. The millions of dried specimens in museums represent a valuable source of RNA for reconstructing historic virus-host interactions[14,15]. It is tempting to speculate that the long-term survival of certain RNA

681 might approach that of DNA[72]. It is time to move beyond the incorrect idea that old, dried
682 samples are not a good source of useful RNA.
683
684 **MATERIALS AND METHODS**
685
686 **Sample Collection**
687 *Pinned Specimens:* FoCo-17 *D. melanogaster* were collected and pinned using standard
688 entomological collection techniques with storage at room temperature or stored frozen at -80°C
689 [73]. Poza Rica *Aedes aegypti* mosquitoes were reared using standard lab techniques until
690 adulthood[74]. Prior to blood feeding mosquitoes were collected and pinned or frozen.
691
692 *Museum Specimens:* Samples were obtained from museums and other institutions containing
693 entomological specimens located in the United States of America and Canada. Altogether, 46
694 drosophilid samples, mainly *D. melanogaster* or *D. simulans*, were selected for the study.
695 Museum species assignments were checked using molecular data as described below. One
696 sample from California, California_2000_2, was initially identified as *D. melanogaster*, but our
697 sequence data indicated that it was *D. simulans* (these species can be difficult to distinguish
698 morphologically). Location, date of sample collection, sample storage type, extraction method,
699 RNA quality and RNA extraction concentration are summarized in **Figure 2**, **Table**
700 **1** and **Supplemental Table 1**
701
702 **Sample Workflow**
703 Deliberate protocols were used to minimize contamination during sample processing and library
704 construction. Sample processing and library construction moved from dedicated pre-PCR rooms
705 to a post-PCR room. RNA extractions were performed in a dedicated pre-PCR sample
706 extraction room in a Class II type B2 biosafety cabinet which protects both personnel and
707 samples. Initial library preparation steps, including reverse transcription, ligation, and setup of
708 library amplification reactions were completed in a separate PCR setup room in an AirClean
709 PCR workstation equipped with a HEPA filter (AirClean Systems, AC600 Series). Finally, library
710 amplification and subsequent cleanup and pooling steps were performed in a third post-PCR lab
711 space.
712
713 **RNA Extraction**

714 *Non-Destructive Sampling:* For samples for which destructive sampling was prohibited, we
715 adapted the protocol described by Santos et. al., 2018[35]. Briefly, individual samples were placed
716 in a PCR tube containing 200µL of solution containing 200mM Tris HCl, 250mM NaCl, 25mM
717 EDTA, 0.5% SDS and 400 µg/mL proteinase K. Samples were then incubated at 56°C for 16
718 hours. After incubation the supernatant was moved to a new tube for RNA isolation and the
719 specimen was transferred to a cryovial containing 80% ethanol. RNA was purified using the
720 Zymo RNA Clean & Concentrator Kit as described below.
721
722 *Ethanol Stored Sample Rehydration:* Four samples arrived in 70% ethanol. To prepare these
723 samples for extraction, each specimen was rehydrated using a gradient of decreasing
724 concentrations of ethanol. The specimens were suspended in 200µL 70%, 50%, 30% and 10%
725 ethanol for 15 minutes on ice with agitation every 2-3 minutes prior to a final incubation in water
726 for 15 minutes before RNA extraction following the destructive sampling method described
727 below.
728
729 *Destructive Sampling:* A phenol/chloroform approach with mechanical disruption was used for
730 RNA isolation of the experimentally dried and frozen samples as well as the museum
731 specimens that could be destructively sampled. Briefly, each specimen was placed in a 2.0mL
732 tube with a small BB (McMaster Carr, 1598K22) and 500µL of Trizol was added and incubated
733 for 5 minutes. Tubes were then shaken in a TissueLyser (Qiagen, 9003240.) at 30 Hz for 3
734 minutes. 100µL of chloroform was added, thoroughly mixed and incubated for two minutes prior
735 to being spun at 12,000xg for 10 minutes. The aqueous phase was retained for RNA purification
736 using the Zymo RNA Clean & Concentrator-5 kit following manufacturer directions for the
737 capture of small RNA fragments with slight modification (Zymo Research, R1013). Briefly,
738 225µL of sample was mixed with 225µL 100% ethanol and 225µL RNA binding buffer. Samples
739 were transferred to spin columns with collection tubes and spun. To capture small RNAs, the
740 flow through from the first spin was retained and mixed with an equal amount of 100% ethanol.
741 This was transferred to the spin column and centrifuged. A wash using RNA wash buffer was
742 done prior to a DNAse treatment following manufacturer recommendations (Zymo Research,
743 E1010). After DNAse treatment, two more washes were complete prior to elution in 30µL of
744 nuclease free water. All spins were performed at 9,000xg for 1 minute unless otherwise noted.
745 For all extraction types, FoCo-17 male and female flies were used as a positive control and an
746 empty tube was used as a negative control.
747

748 **RNA Quality and Quantification**
749 RNA quality was assessed using a nanodrop spectrophotometer (Thermo Scientific
750 ND2000USCAN) and RNA concentration was determined using the Qubit high-sensitivity RNA
751 reagent (ThermoFisher, Q32852). RNA length was measured using the Agilent Tapestation
752 High Sensitivity RNA screening tapes and reagents (Agilent, 5067-5579 & 5067-5580).
753
754 **RT-qPCR**
755 *Pinned Samples:* Several targets were assessed for presence/absence and evidence of
756 degradation using RT-qPCR (primer sequences in **Supplemental Table 3**). cDNA was
757 generated using 5.5µL RNA, 10µM random hexamer primers (IDT), 10µM dNTPs and water to
758 13µL and incubated at 65°C for 5 minutes. Next, 4µL 5X FS buffer, 1µL 0.1M DTT and 1µL
759 reverse transcriptase was added and incubated at 50°C for 60 minutes followed by a heat
760 inactivation step at 80°C for 10 minutes after which each sample was diluted in 90µL nuclease-
761 free water. qPCR was conducted using NEB Luna Universal qPCR Mastermix following
762 manufacturer recommendations and cycling conditions (NEB, M3003).
763
764 **PCR controls**
765 RNA from a pool of FoCo-17 flies was reverse transcribed to create a cDNA positive control for
766 fly samples. For mosquito RT-qPCR, positive control cDNA was reverse transcribed from
767 individual colony mosquitoes. We included these positive controls and three negative controls
768 in all qPCR runs. Negative controls consisted of an extraction blank (a no sample extraction), a
769 no-sample RT control, and a no template qPCR control. The use of negative controls at each
770 step would have allowed us to determine when cross-contamination had been introduced if it
771 had been. Positive/negative status was determined using the melt curve (within 1 degree of the
772 positive control) for each sample and target. Agarose gel electrophoresis of qPCR products was
773 used to determine positive/negative status when Ct and melt curve were ambiguous.
774
775 *Museum Collections:* We used RT-qPCR to determine if any samples had detectable levels of
776 galbut virus RNA and RpL32 mRNA. To increase our ability to detect highly fragmented RNA,
777 we designed a second set of primer that target a small region of the galbut virus RNA 1 and *D.*
778 *melanogaster* mRNA RpL32. A 2% ethidium bromide agarose gel was used to confirm
779 positive/negative status. Galbut virus positive female and male FoCo-17 flies were used as
780 positive controls and water was used as a negative control.
781 **Supplemental Table 3: Primer sequences used in this study.**

Primer pair name (#s in lab collection)	Forward	Reverse	Reference
Galbut virus (long) (#1600/1601)	CCGTGAAGCAAGGAATCAAT	TGCCGATTTTCTGCTCTTTT	[30]
Galbut virus-short (1948/1949)	AGAAGATGTGCTGTAGTGACAC	CGTGGAATTCCGAACGGCTA	This study
RpL32- long (1012/1013)	TGCTAAGCTGTCGCACAAATGG	TGCGCTTGTTCGATCCGTAAC	[75]
RpL32- short (1950/1951)	GCGCTTGTTCGATCCGTAAC	GCCGCTTCAAGGGACAGTAT	This study
Thika virus (1604/1605)	CAGCAGGTCCCTTGCTAAAG	TGGTCAGCATATGACCGAAA	[30]
Nora virus (1592/1593)	GCACCTGGTCGATTGAATCC	CGTTCAGGGCATAGTCAAGC	[30]
La Jolla virus (1692/1693)	ACCGTATGGCGTCGTACTTC	AAAGTATCAGCAGCGCGAAT	[30]
Actin (#1826/1827)	CGTTCGTGACATCAAGGAAA	GAACGATGGCTGGAAGAGAG	[76]
Verdadero virus (#1662/1663)	ATATGGGTCGTGTCGAAAGC	CACCCCGAAATTTTCTTCAA	[30]
Guadeloupe mosquito virus (#1688/1689)	TTGTAAATCCCCCTGTGCTC	CGCAAAAATTGGGTTTGAGT	This study

782

783 **NGS Library Preparation**

784 Museum collection samples were prepared for sequencing using the Kapa Biosystems Kapa
785 RNA Hyper Prep kit following manufacturer recommendations with modification of the
786 fragmentation/priming step. Since the RNA was already highly fragmented, samples were
787 minimally incubated at 65°C for 1 minute during the fragmentation/priming step (Roche,
788 08098093702). Due to low starting concentrations, 12 cycles were used for library amplification.
789 FoCo-17 fly RNA was used as a positive control and water was used as a negative control for
790 library preparation and sequencing. Controls were sequenced on a separate run to avoid index
791 hopping from the positive control sample[77]. Sample pooling was determined using High
792 Sensitivity DNA Qubit reagents and final library quality control was done using an Agilent D1000
793 HS Tapestation and KapaQuant reagents following manufacturers recommendations (Roche,

794 07960140001). Museum samples were sequenced on three NextSeq 500 runs; one high output
795 75 cycle run and two mid output 150 cycle runs. All museum specimens were run on the first
796 NextSeq run, runs two and three consisted of samples that we wanted to increase coverage of
797 near complete virus sequences. Experimentally dried samples were sequenced on a high output
798 75 cycle run. The two positive control samples were sequenced on a 300 cycle MiSeq run.
799 Additional fresh frozen samples were sequenced on a NextSeq mid output 150 cycle kit.
800
801 **Data Analysis**
802
803 *Experimental Collections:* All statistical analysis and data visualization, unless otherwise noted,
804 was done using R/RStudio. Data cleaning and data visualization were done using the tidyverse
805 package[78]. All scripts are available in the GitHub repository linked below. A p-value of $\alpha = 0.05$
806 or below was used as our significance threshold. RNA Concentration and Length: Four
807 individual multiple linear regression models (MLRs) were constructed to test for statistical
808 significance in RNA concentration and length between dried and frozen flies and mosquitoes
809 over 72- and 52-weeks. The predictor time was treated as a continuous variable and the
810 predictor storage type was converted to factor. A balanced one-way analysis of variance
811 (ANOVA) was used to test for significance using the car package[79]. The performance package
812 was used to test model assumptions[80]. RT-qPCR: Raw qPCR data files were cleaned and
813 compiled using the SangerTools R package and a custom R script[81]. Two-tailed Students T-
814 tests from the rstatix package were used to determine statistical significance of dried and frozen
815 Ct values[82]. P-values were adjusted for multiple hypothesis testing.
816
817 *Identification of virus sequences in old samples:* We used our lab's previously described
818 metagenomic classification pipeline (https://github.com/stenglein-lab/taxonomy_pipeline) to
819 identify and validate virus sequences in NGS datasets[30]. In brief, adapters and low quality reads
820 were trimmed using cutadapt 3.5[83]. Fastqc was used to assess post-collapsed read
821 quality 0.11.9[84]. Host reads were removed using bowtie2 2.4.5 and the remaining reads were
822 assembled using spades 3.15.4[85,86]. Virus sequences were identified using BLASTn 2.12.0 and
823 a BLASTx search using diamond 2.0.14 was used to identify novel sequences[87,88]. Draft
824 sequences were validated by remapping of trimmed reads using bwa mem aligner version
825 0.7.17[89]. Final sequences were submitted to the NCBI nucleotide database and raw NGS data
826 to the NCBI sequence read archive repository.
827

828 This metagenomic classification pipeline was also used to taxonomically assign non-host
829 contigs and unassembled reads. Counts assigned to individual taxa were normalized to the
830 number of quality- and adapter-trimmed reads.
831
832 *Molecular species identification using cytochrome oxidase subunit 1 competitive mapping.* The
833 sequence of this mitochondrial-encoded gene is commonly used to distinguish related
834 species[90]. We used the *D. melanogaster* CO1 coding sequence from NC_024511 as a BLASTN
835 query to the NCBI nucleotide database to identify other drosophilid CO1 sequences[91]. We
836 restricted results to sequences from Drosophilidae and to alignments with >90% query coverage
837 and E-value $<1x10^{-50}$. We used cd-hit-est to collapse sequences that shared >99% pairwise
838 nucleotide identity to create a set of 545 representative CO1 sequences[92]. We mapped adapter
839 and quality trimmed reads to these sequences using bowtie2 v.2.4.4 in end-to-end mode and
840 retained alignments with a mapping quality ≥ 20.
841
842 *Maximum Likelihood Trees:* All available galbut virus and sigma virus sequences from individual
843 flies (and not pools) with collection date metadata were downloaded from GenBank. Sequences
844 in the Puslinch virus phylogeny include all available L protein sequences in the NCBI RefSeq
845 protein database from the *Peribunyaviridae* family. Sequences in the sobemo-like virus tree
846 include RdRp protein sequences from viral genomes identified by a BLASTN search of the
847 NCBI nucleotide database. Alignments were generated using MAFTT v7.490 with default
848 parameters. IqTree v1.0 (http://iqtree.cibiv.univie.ac.at) was used to generate maximum
849 likelihood trees[93]. The following parameters were used on the web interface version of IqTree:
850 substitution model- auto, Free-rate Heterogeneity- yes, bootstrap analysis- ultrafast with all
851 other options set to default. FigTree was used for tree visualization
852 (http://tree.bio.ed.ac.uk/software/figtree/). Trees were midpoint rooted.
853
854 *Analysis of strandedness of virus-mapping reads.* To tabulate the numbers of positive and
855 negative strand reads mapping to virus sequences, we mapped quality- and adapter-trimmed
856 reads to assembled virus sequences using the bwa mem aligner version 0.7.17[89]. The
857 orientation of each mapped read was determined from the 0x10 bit flag of the resulting sam
858 format output.
859
860 For all analyses of virus- and host -mapping reads, values were summarized and visualized
861 using the tidyverse R packages[78]. Wilcoxon tests were used to statistically evaluate differences

between groups using the rstatix R package. In all cases values were determined to be non-normally distributed by Shapiro-Wilk test[82]. *P*-values were adjusted for multiple testing using the Holm–Bonferroni method and were indicated on plots using the ggpubr R package using the following significance levels: ns: p > 0.05; *: p <= 0.05; **: p <= 0.01; ***: p <= 0.001; ****: p <= 0.0001[94]. Analyes were implemented as nextflow workflows available at: https://github.com/LKeene/Old_Collections_Figures/[95].

Analysis of ribosomal rRNA-mapping reads. Adapter- and quality-trimmed reads from *D. melanogaster* datasets were mapped to the 18S and 28S rRNA sequences from Anger et al (chains B5 and A2 from[54]) using bwa mem aligner version 0.7.17[89]. Per-base, per-strand coverage was calculated using the BamToCov tool v2.7.0[96]. The *D. melanogaster* 80S ribosome structure was visualized using ChimeraX v.1.7.1[97]. Bases were binned into one of four categories (paired, non-paired, higher-order structure, absent from structure) by feeding this structure (protein data bank accession 4V6W) into RNApdbee 2.0[55].

*Analysis of non-ribosomal RNA types. A*dapter- and quality-trimmed reads from *D. melanogaster* datasets were mapped to the *D. melanogaster* genome version BDGP6.32[98] using bwa mem aligner version 0.7.17[89]. Mapping output and genome annotation were input into ALFA v1.1.1 to tabulate the fractions of reads mapping to each of the annotated genomic biotypes[57].

Analysis of mismatch signatures of chemical damage. Trimmed reads from *D. melanogaster* datasets were mapped to rRNA as above. Mismatches of bases with a basecall quality score >30 were tabulated.

Competitive mapping to ribosomal internal transcribed spacer sequences. We collected sequences between the 18S and 5.8S rRNA genes for the four museum species. Sequences correspond to Genbank accessions: *D. melanogaster*: NR_133558.1:2861-722; *D. simulans*: NGVV02000020.1:5755-5071; *D. putrida*: AF184042.1:153-611; *S. pallida*: JAECXP010000218.1:7393-7904. We mapped adapter and quality trimmed reads to these sequences using bowtie2 v.2.4.4 in end-to-end mode and retained alignments with a mapping quality ≥ 30.

ACKNOWLEDGEMENTS

The authors would like to acknowledge the museum institutions and staff for their willingness to share specimens for this work: Robin Thomson, University of Minnesota Insect Collection; Timothy McCabe, New York State Museum; Chris Paradise, The Davidson College Entomology Collection; Matt Gimmel, Santa Barbara Museum of Natural History; Camiel Doorenweerd, University of Hawaii Insect Museum; Jayme Sones, The Centre for Biodiversity and Genomics at the University of Guelph; Laura Porturas, The Frost Entomology Center at Pennsylvania State University; Tommy McElrath, Illinois Natural History Survey. The authors would also like to thank Dr. Brian Foy for providing *Ae. aegypti* mosquitoes, and Dr. Rebekah Kading for the supplies to pin and store dried insects. We thank Darren Obbard, Dan Sloan, and Jeff Wilusz for helpful discussions.

FUNDING: NSF IOS 2048214 (MDS), NIH T32GM132057 (AHK), Computational resources supported by NIH/NCATS Colorado CTSA Grant Number UL1 TR002535

DATA AVAILABILITY

All metadata, RT-qPCR raw data, plots, and analysis and visualization code can be found at: https://github.com/LKeene/Old_Collections_Figures. Raw sequence data has been uploaded to the NCBI SRA database; assembled viral sequences have been deposited in GenBank; both can be found under NCBI BioProject accession PRJNA1034757.

REFERENCES

1. Leonardi, M. *et al.* Evolutionary Patterns and Processes: Lessons from Ancient DNA. *Syst Biol* **66**, syw059 (2016).
2. Orlando, L. & Cooper, A. Using ancient DNA to understand evolutionary and ecological processes. *Annu Rev Ecol Evol Syst* **45**, 573–598 (2014).
3. Green, R. E. *et al.* A draft sequence of the neandertal genome. *Science (1979)* **328**, 710–722 (2010).
4. Duchêne, S., Ho, S. Y. W., Carmichael, A. G., Holmes, E. C. & Poinar, H. The Recovery, Interpretation and Use of Ancient Pathogen Genomes. *Current Biology* **30**, R1215–R1231 (2020).
5. Ng, T. F. F. *et al.* Preservation of viral genomes in 700-y-old caribou feces from a subarctic ice patch. *Proc Natl Acad Sci U S A* **111**, 16842–7 (2014).
6. Fromm, B. *et al.* Ancient microRNA profiles of 14,300-yr-old canid samples confirm taxonomic origin and provide glimpses into tissue-specific gene regulation from the Pleistocene. *RNA* **27**, 324–334 (2021).
7. Faria, N. R. *et al.* The early spread and epidemic ignition of HIV-1 in human populations. *Science (1979)* **346**, 56–61 (2014).
8. Taubenberger, J. K., Reid, A. H., Krafft, A. E., Bijwaard, K. E. & Fanning, T. G. Initial Genetic Characterization of the 1918 “Spanish” Influenza Virus. *Science (1979)* **275**, 1793–1796 (1997).

9. Belyi, V. A., Levine, A. J. & Skalka, A. M. Sequences from Ancestral Single-Stranded DNA Viruses in Vertebrate Genomes: the Parvoviridae and Circoviridae Are More than 40 to 50 Million Years Old . *J Virol* **84**, 12458–12462 (2010).
10. Ávila-Arcos, M. C. *et al.* One hundred twenty years of koala retrovirus evolution determined from museum Skins. *Mol Biol Evol* **30**, 299–304 (2013).
11. Enard, D. & Petrov, D. A. Ancient RNA virus epidemics through the lens of recent adaptation in human genomes. *Philosophical Transactions of the Royal Society B: Biological Sciences* **375**, 20190575 (2020).
12. Yang, E. *et al.* Decay rates of human mRNAs: correlation with functional characteristics and sequence attributes. *Genome Res* **13**, 1863–72 (2003).
13. Fordyce, S. L., Kampmann, M.-L., van Doorn, N. L. & Gilbert, M. T. P. Long-term RNA persistence in postmortem contexts. *Investig Genet* **4**, 7 (2013).
14. Smith, O. *et al.* A complete ancient RNA genome: Identification, reconstruction and evolutionary history of archaeological Barley Stripe Mosaic Virus. *Sci Rep* **4**, 4003 (2014).
15. Peyambari, M., Warner, S., Stoler, N., Rainer, D. & Roossinck, M. J. A 1,000-Year-Old RNA Virus. *J Virol* **93**, e01188-18 (2019).
16. Mármol-Sánchez, E. *et al.* Historical RNA expression profiles from the extinct Tasmanian tiger. *Genome Res* **33**, 1299–1316 (2023).
17. Cobb, N. S. *et al.* Assessment of North American arthropod collections: prospects and challenges for addressing biodiversity research. *PeerJ* **7**, e8086 (2019).
18. Watts, P. C., Thompson, D. J., Allen, K. A. & Kemp, S. J. How useful is DNA extracted from the legs of archived insects for microsatellite-based population genetic analyses? *J Insect Conserv* **11**, 195–198 (2007).
19. Heintzman, P. D., Elias, S. A., Moore, K., Paszkiewicz, K. & Barnes, I. Characterizing DNA preservation in degraded specimens of Amara alpina (Carabidae: Coleoptera). *Mol Ecol Resour* **14**, 606–615 (2014).
20. Goldstein, P. Z. & Desalle, R. Calibrating phylogenetic species formation in a threatened insect using DNA from historical specimens. *Mol Ecol* **12**, 1993–1998 (2003).
21. Tin, M. M.-Y., Economo, E. P. & Mikheyev, A. S. Sequencing Degraded DNA from Non-Destructively Sampled Museum Specimens for RAD-Tagging and Low-Coverage Shotgun Phylogenetics. *PLoS One* **9**, e96793 (2014).
22. Lalonde, M. M. L. & Marcus, J. M. How old can we go? Evaluating the age limit for effective DNA recovery from historical insect specimens. *Syst Entomol* **45**, 505–515 (2020).
23. Gilbert, M. T. P., Moore, W., Melchior, L. & Worobey, M. DNA Extraction from Dry Museum Beetles without Conferring External Morphological Damage. *PLoS One* **2**, e272 (2007).
24. Shpak, M., Ghanavi, H. R., Lange, J. D., Pool, J. E. & Stensmyr, M. C. Genomes from historical Drosophila melanogaster specimens illuminate adaptive and demographic changes across more than 200 years of evolution. *PLoS Biol* **21**, e3002333 (2023).
25. Webster, C. L., Longdon, B., Lewis, S. H. & Obbard, D. J. Twenty-Five New Viruses Associated with the Drosophilidae (Diptera). *Evolutionary Bioinformatics* **12s2**, EBO.S39454 (2016).
26. Webster, C. L. *et al.* The Discovery, Distribution, and Evolution of Viruses Associated with Drosophila melanogaster. *PLoS Biol* **13**, e1002210 (2015).
27. Yamaguchi, M. & Yoshida, H. Drosophila as a Model Organism. in *Advances in Experimental Medicine and Biology* vol. 1076 1–10 (Springer New York LLC, 2018).
28. Beckingham, K. M., Armstrong, J. D., Texada, M. J., Munjaal, R. & Baker, D. A. Drosophila melanogaster--the model organism of choice for the complex biology of multi-cellular organisms. *Gravit Space Biol Bull* **18**, 17–29 (2005).

29. Longdon, B., Wilfert, L. & Jiggins, F. M. *The Sigma Viruses of Drosophila from: Rhabdoviruses: Molecular Taxonomy, Evolution, Genomics, Ecology, Host-Vector Interactions, Cytopathology and Control*. (Caister Academic Press, U.K., 2012).
30. Cross, S. T. *et al.* Partitiviruses Infecting Drosophila melanogaster and Aedes aegypti Exhibit Efficient Biparental Vertical Transmission. *J Virol* **94**, (2020).
31. Vera-Maloof, F. Z., Saavedra-Rodriguez, K., Elizondo-Quiroga, A. E., Lozano-Fuentes, S. & Black Iv, W. C. Coevolution of the Ile1,016 and Cys1,534 Mutations in the Voltage Gated Sodium Channel Gene of Aedes aegypti in Mexico. *PLoS Negl Trop Dis* **9**, e0004263 (2015).
32. Ortiz-Baez, A. S., Shi, M., Hoffmann, A. A. & Holmes, E. C. RNA virome diversity and Wolbachia infection in individual Drosophila simulans flies. *J Gen Virol* **102**, 001639 (2021).
33. Habayeb, M. S., Ekengren, S. K. & Hultmark, D. Nora virus, a persistent vitus in Drosophila, defines a new picorna-like virus family. *Journal of General Virology* **87**, 3045–3051 (2006).
34. Shi, C. *et al.* Stable distinct core eukaryotic viromes in different mosquito species from Guadeloupe, using single mosquito viral metagenomics. *Microbiome* **7**, 121 (2019).
35. Santos, D., Ribeiro, G. C., Cabral, A. D. & Sperança, M. A. A non-destructive enzymatic method to extract DNA from arthropod specimens: Implications for morphological and molecular studies. *PLoS One* **13**, e0192200 (2018).
36. Sturtevant, A. H. A New Species Closely Resembling *Drosophila Melanogaster*. *Psyche (Camb Mass)* **26**, 153–155 (1919).
37. Sturtevant, A. H. Notes on North American Drosophilidae with Descriptions of Twenty-Three New Species. *Ann Entomol Soc Am* **9**, 323–343 (1916).
38. Cross, S. T. *et al.* Co-Infection Patterns in Individual Ixodes scapularis Ticks Reveal Associations between Viral, Eukaryotic and Bacterial Microorganisms. *Viruses* **10**, 388 (2018).
39. Hoskins, R. A. *et al.* The Release 6 reference sequence of the Drosophila melanogaster genome. *Genome Res* **25**, 445–58 (2015).
40. Kim, B. Y. *et al.* Single-fly genome assemblies fill major phylogenomic gaps across the Drosophilidae Tree of Life. *PLoS Biol* **22**, e3002697 (2024).
41. Balique, F., Colson, P. & Raoult, D. Tobacco mosaic virus in cigarettes and saliva of smokers. *Journal of Clinical Virology* **55**, 374–376 (2012).
42. Kircher, M., Sawyer, S. & Meyer, M. Double indexing overcomes inaccuracies in multiplex sequencing on the Illumina platform. *Nucleic Acids Res* **40**, e3 (2012).
43. Rambaut, A., Lam, T. T., Max Carvalho, L. & Pybus, O. G. Exploring the temporal structure of heterochronous sequences using TempEst (formerly Path-O-Gen). *Virus Evol* **2**, vew007 (2016).
44. Aiewsakun, P. & Katzourakis, A. Time-Dependent Rate Phenomenon in Viruses. *J Virol* **90**, 7184–7195 (2016).
45. Ghafari, M., Simmonds, P., Pybus, O. G. & Katzourakis, A. A mechanistic evolutionary model explains the time-dependent pattern of substitution rates in viruses. *Current Biology* **31**, 4689-4696.e5 (2021).
46. Drummond, A., Pybus, O. G. & Rambaut, A. Inference of viral evolutionary rates from molecular sequences. *Adv Parasitol* **54**, 331–58 (2003).
47. Duchêne, S., Holmes, E. C. & Ho, S. Y. W. Analyses of evolutionary dynamics in viruses are hindered by a time-dependent bias in rate estimates. *Proceedings of the Royal Society B: Biological Sciences* **281**, 20140732 (2014).
48. Cross, S. T. *et al.* Galbut Virus Infection Minimally Influences Drosophila melanogaster Fitness Traits in a Strain and Sex-Dependent Manner. *Viruses* **15**, 539 (2023).

1035 49. Wallace, M. A. *et al.* The discovery, distribution, and diversity of DNA viruses associated
1036 with *Drosophila melanogaster* in Europe. *Virus Evol* **7**, veab031 (2021).
1037 50. Lowen, A. C. It's in the mix: Reassortment of segmented viral genomes. *PLoS Pathog* **14**,
1038 e1007200 (2018).
1039 51. Parkhomchuk, D. *et al.* Transcriptome analysis by strand-specific sequencing of
1040 complementary DNA. *Nucleic Acids Res* **37**, e123 (2009).
1041 52. Nibert, M. L. *et al.* Taxonomic reorganization of family Partitiviridae and other recent
1042 progress in partitivirus research. *Virus Res* **188**, 128–41 (2014).
1043 53. Robicheau, B. M., Susko, E., Harrigan, A. M. & Snyder, M. Ribosomal RNA genes
1044 contribute to the formation of pseudogenes and junk DNA in the human genome.
1045 *Genome Biol Evol* **9**, 380–397 (2017).
1046 54. Anger, A. M. *et al.* Structures of the human and Drosophila 80S ribosome. *Nature* **497**,
1047 80–5 (2013).
1048 55. Zok, T. *et al.* RNApdbee 2.0: multifunctional tool for RNA structure annotation. *Nucleic*
1049 *Acids Res* **46**, W30–W35 (2018).
1050 56. Staple, D. W. & Butcher, S. E. Pseudoknots: RNA structures with diverse functions. *PLoS*
1051 *Biol* **3**, e213 (2005).
1052 57. Bahin, M. *et al.* ALFA: annotation landscape for aligned reads. *BMC Genomics* **20**, 250
1053 (2019).
1054 58. Sharp, S. J., Schaack, J., Cooley, L., Burke, D. J. & Söll, D. Structure and transcription of
1055 eukaryotic tRNA genes. *CRC Crit Rev Biochem* **19**, 107–44 (1985).
1056 59. Zhang, J. Recognition of the tRNA structure: Everything everywhere but not all at once.
1057 *Cell Chem Biol* **31**, 36–52 (2024).
1058 60. Dabney, J., Meyer, M. & Pääbo, S. Ancient DNA damage. *Cold Spring Harb Perspect Biol*
1059 **5**, a012567 (2013).
1060 61. Shibutani, S., Takeshita, M. & Grollman, A. P. Insertion of specific bases during DNA
1061 synthesis past the oxidation-damaged base 8-oxodG. *Nature* **349**, 431–4 (1991).
1062 62. Sloan, D. B., Broz, A. K., Sharbrough, J. & Wu, Z. Detecting Rare Mutations and DNA
1063 Damage with Sequencing-Based Methods. *Trends Biotechnol* **36**, 729–740 (2018).
1064 63. Rhee, Y., Valentine, M. R. & Termini, J. Oxidative base damage in RNA detected by
1065 reverse transcriptase. *Nucleic Acids Res* **23**, 3275–82 (1995).
1066 64. Sinha, R. *et al.* Index switching causes 'spreading-of-signal' among multiplexed samples
1067 in Illumina HiSeq 4000 DNA sequencing. doi:10.1101/125724.
1068 65. Valentine, M. R. & Termini, J. Kinetics of formation of hypoxanthine containing base pairs
1069 by HIV-RT: RNA template effects on the base substitution frequencies. *Nucleic Acids Res*
1070 **29**, 1191–9 (2001).
1071 66. Zhang, K., Hodge, J., Chatterjee, A., Moon, T. S. & Parker, K. M. Duplex structure of
1072 double-stranded RNA provides stability against hydrolysis relative to single-stranded
1073 RNA. *Environ Sci Technol* **55**, 8045–8053 (2021).
1074 67. Sandoval-Velasco, M. *et al.* Three-dimensional genome architecture persists in a 52,000-
1075 year-old woolly mammoth skin sample. *Cell* **187**, 3541-3562.e51 (2024).
1076 68. Petrzik, K. Evolutionary forces at work in partitiviruses. *Virus Genes* **55**, 563–573 (2019).
1077 69. Skoglund, P. *et al.* Separating endogenous ancient DNA from modern day contamination
1078 in a Siberian Neandertal. *Proc Natl Acad Sci U S A* **111**, 2229–2234 (2014).
1079 70. Laurence, M., Hatzis, C. & Brash, D. E. Common contaminants in next-generation
1080 sequencing that hinder discovery of low-abundance microbes. *PLoS One* **9**, e97876
1081 (2014).
1082 71. Naccache, S. N. *et al.* The perils of pathogen discovery: origin of a novel parvovirus-like
1083 hybrid genome traced to nucleic acid extraction spin columns. *J Virol* **87**, 11966–77
1084 (2013).

72. Kjær, K. H. *et al.* A 2-million-year-old ecosystem in Greenland uncovered by environmental DNA. *Nature* **612**, 283–291 (2022).
73. Krogmann, L. & Holstein, J. *Chapter 18 Preserving and Specimen Handling: Insects and Other Invertebrates*. vol. 8 (ABC TAXA, 2010).
74. Foster, W. A. Colonization and Maintenance of Mosquitoes in the Laboratory. in *Pathology, Vector Studies, and Culture* 103–151 (Elsevier, 1980). doi:10.1016/B978-0-12-426102-0.50009-9.
75. Cao, C., Magwire, M. M., Bayer, F. & Jiggins, F. M. A Polymorphism in the Processing Body Component Ge-1 Controls Resistance to a Naturally Occurring Rhabdovirus in Drosophila. *PLoS Pathog* **12**, e1005387 (2016).
76. Dzaki, N., Ramli, K. N., Azlan, A., Ishak, I. H. & Azzam, G. Evaluation of reference genes at different developmental stages for quantitative real-time PCR in Aedes aegypti. *Sci Rep* **7**, 43618 (2017).
77. van der Valk, T., Vezzi, F., Ormestad, M., Dalén, L. & Guschanski, K. Index hopping on the Illumina HiseqX platform and its consequences for ancient DNA studies. *Mol Ecol Resour* **20**, 1171–1181 (2020).
78. Wickham, H. *et al.* Welcome to the Tidyverse. *J Open Source Softw* **4**, 1686 (2019).
79. Fox, J. & Weisberg, S. *An R Companion to Applied Regression*. (Sage, 2019).
80. Lüdecke, D., Ben-Shachar, M., Patil, I., Waggoner, P. & Makowski, D. performance: An R Package for Assessment, Comparison and Testing of Statistical Models. *J Open Source Softw* **6**, 3139 (2021).
81. Laldin, A. & Hutson, G. SangerTools: Tools for Population Health Management Analytics. (2022).
82. Kassambara, A. rstatix: Pipe-Friendly Framework for Basic Statistical Tests. *https://rpkgs.datanovia.com/rstatix/* (2023).
83. Martin, M. Cutadapt Removes Adapter Sequences From High-Throughput Sequencing Reads. *EMBnet J* **17**, 10–12 (2011).
84. Andrews, S. *et al.* FastQC: a quality control tool for high throughput sequence data. https://qubeshub.org/resources/fastqc (2012).
85. Langmead, B. & Salzberg, S. L. Fast gapped-read alignment with Bowtie 2. *Nat Methods* **9**, 357–359 (2012).
86. Prjibelski, A., Antipov, D., Meleshko, D., Lapidus, A. & Korobeynikov, A. Using SPAdes De Novo Assembler. *Curr Protoc Bioinformatics* **70**, e102 (2020).
87. Buchfink, B., Reuter, K. & Drost, H. G. Sensitive protein alignments at tree-of-life scale using DIAMOND. *Nat Methods* **18**, 366–368 (2021).
88. Camacho, C. *et al.* BLAST+: architecture and applications. *BMC Bioinformatics* **10**, 421 (2009).
89. Li, H. & Durbin, R. Fast and accurate long-read alignment with Burrows-Wheeler transform. *Bioinformatics* **26**, 589–595 (2010).
90. Hebert, P. D. N., Ratnasingham, S. & deWaard, J. R. Barcoding animal life: cytochrome c oxidase subunit 1 divergences among closely related species. *Proc Biol Sci* **270 Suppl 1**, S96-9 (2003).
91. Morgulis, A. *et al.* Database indexing for production MegaBLAST searches. *Bioinformatics* **24**, 1757–64 (2008).
92. Fu, L., Niu, B., Zhu, Z., Wu, S. & Li, W. CD-HIT: accelerated for clustering the next-generation sequencing data. *Bioinformatics* **28**, 3150–2 (2012).
93. Nguyen, L. T., Schmidt, H. A., Von Haeseler, A. & Minh, B. Q. IQ-TREE: A fast and effective stochastic algorithm for estimating maximum-likelihood phylogenies. *Mol Biol Evol* **32**, 268–274 (2015).
94. Kassambara, A. ggpubr: ‘ggplot2’ Based Publication Ready Plots. R package version 0.6.0. *https://rpkgs.datanovia.com/ggpubr/* (2023).

95. Zhang, J. *et al.* International Cancer Genome Consortium Data Portal--a one-stop shop for cancer genomics data. *Database (Oxford)* **2011**, bar026 (2011).
96. Birolo, G. & Telatin, A. BamToCov: An efficient toolkit for sequence coverage calculations. *Bioinformatics* **38**, 2617–2618 (2022).
97. Meng, E. C. *et al.* UCSF ChimeraX: Tools for structure building and analysis. *Protein Sci* **32**, e4792 (2023).
98. Hoskins, R. A. *et al.* The Release 6 reference sequence of the Drosophila melanogaster genome. *Genome Res* **25**, 445–458 (2015).